HOST UNIVERSITY: The University of Edinburgh

FACULTY: School of Engineering

DEPARTMENT: BRE Centre for Fire Safety Engineering

Academic Year 2017-2018

Tunnel Fire Suppression Systems & Ventilation Design

Looi Khai Chern

Promoter: Dr Ricky Carvel

Master thesis submitted in the Erasmus+ Study Programme

International Master of Science in Fire Safety Engineering

Disclaimer

This thesis is submitted in partial fulfilment of the requirements for the degree of The International Master of Science in Fire Safety Engineering (IMFSE). This thesis has never been submitted for any degree or examination to any other University/programme. The author declares that this thesis is original work except where stated. This declaration constitutes an assertion that full and accurate references and citations have been included for all material, directly included and indirectly contributing to the thesis. The author gives permission to make this master thesis available for consultation and to copy parts of this master thesis for personal use. In the case of any other use, the limitations of the copyright have to be respected, in particular with regard to the obligation to state expressly the source when quoting results from this master thesis. The thesis supervisor must be informed when data or results are used.

Word count: 16115

Read and approved,

Looi Khai Chern

30 April 2018

Abstract

With a few high profile tunnel fire incidents happening in recent years, fire safety has been a serious issue in tunnels. Several tunnel fire safety components have been invented, tested and implemented in many tunnels, however the interactions between these components are not fully studied and understood. This thesis studies the impact of tunnel longitudinal ventilation system together with water mist system on fire by varying a few key parameters.

Fire Dynamics Simulator (FDS), which is a Computational Fluid Dynamics (CFD) software widely used in fire safety engineering field, is used to simulate a full scale heavy good vehicle fire close to jet fans in a 600 m long tunnel, with water mist systems. The vehicle height, number of water nozzles, location of water nozzles, design fire size and water droplet size are all individually studied in order to attempt to have a comprehensive understanding on how these factors affect smoke backlayering, which is the main criteria when designing longitudinal ventilation system.

The result shows that lesser jet fans are required to prevent backlayering when the vehicles are taller, more water nozzles are used, fire size is smaller and water droplet size is smaller. Various cooling mechanisms and tunnel fire dynamics involved in these interactions shall be discussed.

This thesis seeks to serve as a general practical guide when designing tunnel fire safety system by providing an overview of how various factors affect each other. Further research should be conducted to validate the results and to formulate the relationships quantitatively.

Contents

List of Figures

List of Tables

1 Introduction

There are many road tunnels existing, being built and planned to be built around the world. With some road tunnels such as the Lrdal tunnel in Norway extending as far as 24km long, the tunnel fire safety aspect cannot be neglected. According to the French statistics, there will be one or two car fires per kilometre of tunnel for every hundred million cars that pass through the tunnel. Out of every hundred million heavy goods vehicles (HGVs) passing through a tunnel, there will be around eight fires per kilometre of tunnel) only one of which will be serious enough to cause any damage to the tunnel itself. Based on the statistics, it has been estimated that there will be between one and three very serious fires out of every thousand million HGVs per kilometre of tunnel [6].

Combining with a few high profile fire incidents, such as the Mont-Blanc tunnel fire in France/Italy, in 1999, causing 39 deaths and the Funicular tunnel fire in Austria in 2000, causing 155 deaths [7], this issue has undoubtedly caught the attention of public and authorities. The dangers a tunnel fire pose to the users are of the following order:

- Firstly, the visibility will be reduced by smoke depending on the evacuees' location relative to fire and affect the evacuation process;
- Evacuees who could not evacuate on time may be intoxicated by smoke, as tunnel is an enclosed environment and the toxic gas concentration will accumulate over fire in the event of fire;
- Finally, temperature inside the tunnel will rise quickly due to convection and radiation and threaten anyone in the tunnel.

The basic objectives of a tunnel fire safety design system are to ensure safe evacuation of tunnel users in the event of fire, to protect the tunnel structure and to provide tenable access for firefighters. Tunnel Design Centre (CETU) [8] in France ranks the relative impact of the ambient conditions in the tunnel according to different objectives, as summarised in Table 1.1.

Table 1.1: Relative impact of ambient conditions regarding the objectives of life safety strategy

Objective	Visibility	Toxicity	Temperature
Allow self-evacuation	+ + +	+ +	+
Improve the tenability time	+	+ + +	+ +
Ease the action of rescue services	+ +	+	+ + +
Protect the infrastructure	0	0	+ + +

However, although the research on tunnel fire safety has been ongoing for decades, there is generally little to no consensus within the industry on how to put different components of fire safety measures together to form a holistic design. Among the few key components, there has been insufficient research focusing on the interaction between tunnel ventilation system and fixed firefighting system (FFFS) although they are expected to affect the fire and smoke development.

Tunnel ventilation system not only acts during emergency situations, it also provides fresh air during normal traffic operation to prevent accumulation of carbon monoxide and other toxic gas released by road vehicles. It is therefore a convenient and cost efficient approach to utilise the tunnel ventilation devices for smoke control purpose. There are mainly two types of tunnel ventilation systems adopted by the industry: transverse and longitudinal ventilation system. The decision of which system to adopt depends on a few factors such as the tunnel geometry, atmospheric condition and construction cost.

One of the most studied aspects of tunnel fire safety design is the concept of critical ventilation velocity(CVV) [9] [10]. The CVV is defined as the minimum longitudinal ventilation velocity to prevent smoke to move reversely from a fire in the tunnel [11]. The upstream smoke spread against ventilation stream due to buoyancy effects is known as backlayering or smoke backflow [12]. Tenability can be assured at the tunnel upstream if the air flow velocity in the tunnel is beyond the CVV and therefore evacuation can be achieved.

Although theoretically there exists a 'super-critical' velocity at which an increase of fire

size no longer raises the CVV [9], there is little research on the 'throttling' influence of a fire towards physical ventilation system in a tunnel, as characterised experimentally by Lee *et al.* [13] and described numerically by Colella *et al.* [14]. The 'throttling' effect results in more thrust required from the fans for a fire beyond the super-critical fire size compared to a smaller fire. This effect fundamentally changes the design of tunnel ventilation system as the design can no longer only be based on a certain critical fire size. This project aims to discover other factors in tunnel fire safety system which may intensify the throttling effect.

Water mist system (WMS) has gained popularity in recent years due to its environmental and economical benefit. It produces water droplets smaller than 1000 μm in diameter and suppresses fire via the modes of displacement of oxygen, gas phase cooling and attenuation of radiation. There are numerous studies experimentally and numerically demonstrating the effectiveness of WMS suppressing fire and cooling gas temperature in tunnel [8] [15] [16]. However the interaction between longitudinal ventilation system and WMS has not been studied thorougly to prove their effectiveness when implemented together. One of the potential effects WMS will have on the longitudinal ventilation system is the additional mass of water vapour added to the smoke layer. Consequently the ventilation system may face greater resistance due to the water curtains created by the non-evaporating water mist droplets, further worsening the 'throttling' effect, causing more thrust needed from the fans. On the other hand, injected fine water droplets will also enhance gas cooling effect and reduce fire throttling effect. Depending on the water flow rate discharged from the WMS, the additional mass may not be negligible and it could fundamentally change the conventional tunnel fire safety system design ideology.

This project intends to study the problem using Computational Fluid Dynamics (CFD) modelling to attempt to simulate actual conditions to provide a more practical insight to tunnel fire safety system designers and engineers.

1.1 Objectives

The objectives of this thesis are:

- to study the effect of water mist system on ventilation flow.
- to determine the relationship among the number of jet fans required to prevent backlayering, vehicle height, water nozzle location, water droplet size, fire size and number of water mist nozzles activated.
- to determine the worst case scenario and the optimum ways to prevent smoke backlayering from occurring when designing tunnel safety system.

Computational Fluid Dynamics (CFD) modelling is used to simulate the smoke flow movement in tunnel and the simulation result will be used as the basis of analysis. CFD is a cost effective and proven robust tool to simulate fire, especially since the cost of experiment for tunnel fires is incredibly high.

This thesis will first lay out the background theories of tunnel fire dynamics and brief introduction to FFFS and tunnel ventilation system. Secondly, the assessment method, Fire Dynamics Simulator (FDS), is introduced, including its validation, input and output parameters. Subsequently, the results obtained from simulations are analysed via various methods and discussed. Finally, further research directions will be discussed.

2 Overview of Tunnel Fire Dynamics and Fire Safety Designs Components

This chapter provides an overview of several key fire dynamics phenomenas, the fire safety components and the known interactions among themselves related to this project.

2.1 Basic Tunnel Fire Dynamics

Tunnel fire differs from open fire in many ways. Firstly, due to the confined environment, the heat feedback to burning fuels in a tunnel is more significant and it often results in higher burning rate or more volatile particles produced. Some fuels which do not sustain self-combustion under open environment may burn vigorously in a tunnel fire. Secondly, the limited supply of oxygen in a tunnel, limited by the tunnel portals, often leads to fuel-rich burning, which in turn produces more toxic gases such as carbon monoxide. Thirdly, during a tunnel fire, as the smoke plume develops, it interacts with the ventilation flow and generates large amount of turbulence within the narrow space. The interaction may lead to change in flow pattern, such as reverse flow of hot gases and throttling of air [1].

Tunnel fire is also different from compartment fires for a few reasons. The influence of ventilation on the heat release rate and combustion efficiency in a tunnel is not dictated by the ventilation factor, as per compartment fires. Besides that, tunnel fires are not likely to grow to conventional 'flashover' like in compartment fires, as there is significant heat losses from the fire to the surrounding walls and the hot gases can escape the tunnel easily. However when a tunnell ventilation system, which usually has high capacity, is abruptedly activated, the flames may suddenly increase in size and length. As a result the fire may spread forward easily due to the preheated vehicles downstream of the fire because of radiation and convection from hot smoke layer. Finally, smoke layer created in tunnel may move along the tunnel surface, losing heat to the surfaces and consequently lose its buoyancy and stratification if the tunnel is very long. At the

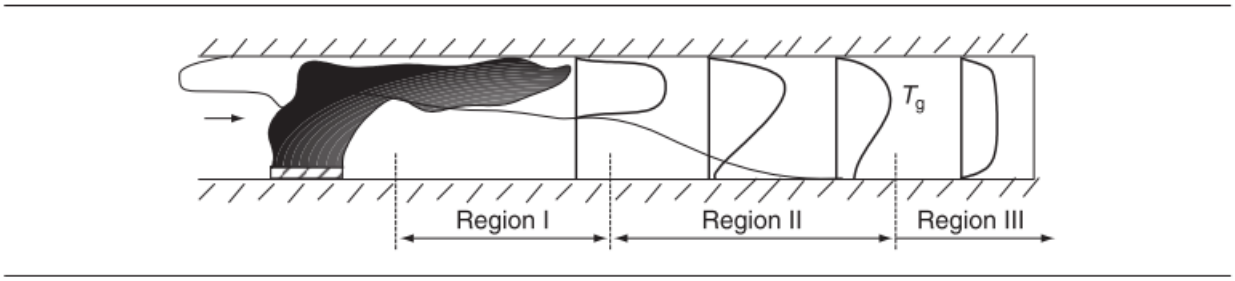

Figure 2.1: Illustration of the three different temperature stratification regions according to Newman [1]

downstream of fire, degree of stratification of the smoke layer depends on the heat losses to the surrounding walls and by the turbulent mixing between the buoyant smoke layer and the cold air moving in opposite direction [1].

Newman [17] defined three distinct regions of temperature stratification using Froude number (Fr), as illustrated in Fig. 2.1.

- Region I, Fr $\leq$ 0.9: stratification is extremely obvious in this region and it is buoyancy-dominated.
- Region II, 0.9 $<$ Fr $\leq$ 10: although there is no strong stratification, there are vertical temperature gradients and there is significant interaction between ventilation velocity and buoyancy induced by fire.
- Region III, Fr $>$ 10: there is no significant temperature gradient in this region.

Fr can be calculated from the equation:

$$Fr = \frac{u_{avg}^2}{1.5(\Delta T_{avg}/T_{avg})gH} \tag{1}$$

where H is the ceiling height, T_{avg} is the average gas temperature (K) over the entire cross-section at a given position, $\Delta T_{avg} = T_{avg} - T_a$ with T_a being the ambient temperature and $u_{avg} = uT_{avg}/T_a$ with u being the flow velocity. Although Newman only divides the degree of stratification into three regions, it can be assumed that within the same region, the higher Fr is, the less stratisfied the smoke layer is.

Vehicles	Experimental HRR		Representative HRR		Experimental HRR with fixed water-based firefighting systems	
	Peak HRR (MW)	Time to Peak HRR (min)	Peak HRR (MW)	Time to Peak HRR (min)	Peak HRR (MW)	Time to Peak HRR (min)
Passenger car	5–10	0–54[a]	5	10	—	—
Multiple passenger car	10–20	10–55[b]	15	20	10–15[g]	35[g]
Bus	25–34[c]	7–14	30	15	20[g,h]	—
Heavy goods truck	20–200[d]	7–48[e]	150	15	15–90[g]	10–30[g]
Flammable/ combustible liquid tanker	200–300	–	300	–	10–200[f]	

Figure 2.2: Fire Data for Typical Vehicles [2]

2.2 Design Fire Size

The most common approach for designers to quantity a fire is through a design fire size, often described in terms of the peak heat release rate (HRR). The HRR in a tunnel fire depends on various factors, including the geometry, vehicles and their contents, and the ventilation conditions [2]. Ingason [2] has summarised the majority of tunnel fire tests carried out around the world over the past few decades. For passenger cars, the peak HRR ranges from 1.5 to 11MW; for buses, the range is between 29 to 34MW; and for heavy good vehicles (HGV), the range is between 13 to 202MW. The time for HGVs to reach the peak HRR is in the range of 10-20 minutes.

Figure 2.2 extracted from NFPA 502 [3] Annex A also tabulates the fire data for typical vehicles, including the experimental HRR, represenatitive HRR and the experimental HRR with fixed water-based firefighting systems.

As seen above, HGVs possess the highest potential HRR and are commonly considered the largest risk in tunnel fire safety design. The wide range of values is due to different test configurations (different materials, ventilation conditions and tunnel geometry) and therefore left up to the designers to prescribe a design value accordingly.

2.3 Tunnel Ventilation System

Tunnel ventilation systems are designed for a few objectives: circulation of air to prevent accumulation of toxic gas emission in the tunnel and for evacuation purpose during emergency. The two main modes of operation of tunnel ventilation systems during a fire are: natural and mechanical ventilation system.

Natural ventilation is typically adopted in 'short' tunnels where it is possible for smoke to be vented due to its buoyancy and pressure differences at the portals. Pressure differences can be present if the slope of the tunnel is significant or if the moving vehicles induce high air velocity, as known as piston effect. The disadvantage of natural ventilation system is apparent when a tunnel is long, as the stratification of smoke layer can be disrupted after a certain distance before smoke vents out to atmosphere, causing the smoke to be recirculated to the fire zone [12]. Eventually the visibility near the fire location will be reduced significantly, causing serious danger to evacuees and firefighters nearby.

Thus, long tunnels are usually equipped with mechanical ventilation systems to ensure the controlled condition inside tunnels. Mechanical ventilation configurations include: longitudinal, fully transverse, semi-transverse and partial transverse. There are some tunnels which incorporate both longitudinal and transverse systems such as the Mont Blanc Tunnel. A ventilation system consists of a combination of fans, ducts and dampers to deliver air to designated locations [12]. NFPA 502 [3] states that emergency ventilation shall not be required in tunnels less than 1000m in length if an engineering analysis can show that the use of natural ventilation can provide level of safety equal or higher than a mechanical ventilation system.

2.3.1 Longitudinal Ventilation System

Longitudinal system is defined by the longitudinal airflow movement along the tunnel initiated either by natural factors (wind, stack effect, piston effect of vehicles) or by fans

(portal fans, shaft fans or jet fans along the tunnel) [18]. The main strategy of such system is to force all the smoke produced to one side of the fire location and prevent backlayering from happening in order to create a smoke free zone for evacuation and fire fighting purpose.

When a fire is started on the floor of a tunnel, hot plume rises above and entrains cold air into the plume. After reaching the ceiling, the plume flows symmetrically in opposite directions along the ceiling. However, when a ventilation flow comes from one direction, the symmetry is broken and the plume is bent by the flow. Consequently, the length of the ceiling jet flowing against the current is reduced. Above a certain velocity, which will be discussed in Section 2.3.3, the plume will only flow in one direction as the propelling force from the ventilation flow is too strong to counter. Figure 2.3 shows tunnel fires 1) without ventilation, 2) with insufficient ventilation to prevent backlayering and 3) with sufficient ventilation to prevent backlayering. The main concern with this system is that there may still be evacuees at the downstream after the ventilation system is activated. Therefore this system is not desirable for tunnels with bidirectional traffic where smoke stratification shall not be disrupted by ventilation system.

2.3.2 Transverse Ventilation System

Transverse ventilation is defined by the transverse airflow movement in the tunnel. The main objective of this type of system is to limit air flow in the longitudinal direction, preserve smoke stratification and extract smoke vertically through either ceiling or floor. Transverse ventilation systems feature the uniform collection and/or distribution of air throughout the length of the tunnel roadway and can be of the full transverse or semi-transverse type [18].

In fully transverse system, fresh air supply and smoke extraction occurs along the tunnel via a system of adjustable louvres servicing two separate plenums. This results in the inflow and outflow of air to be identical volumetrically and the two air streams have a direction transverse to the longitudinal axis of tunnel. In semi-transverse system, there

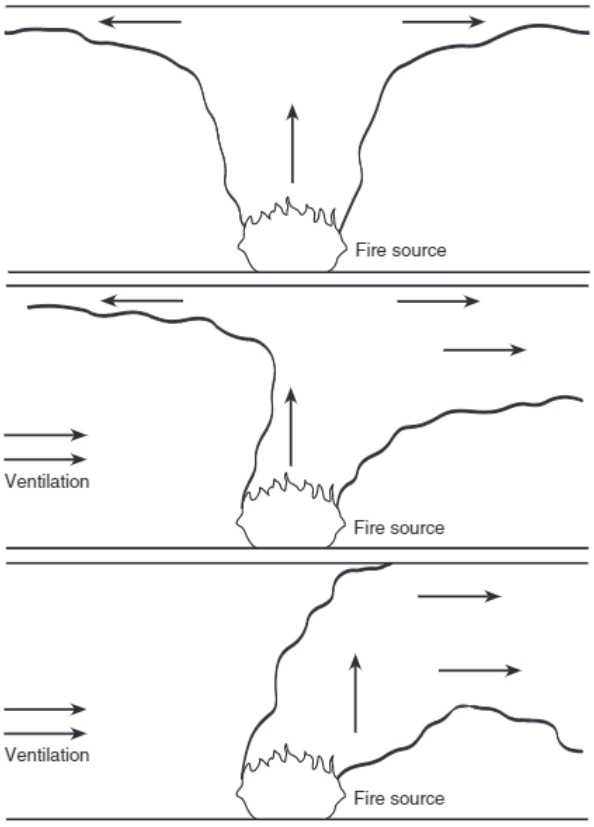

Figure 2.3: Top: Tunnel Fire Without Ventilation; middle: Tunnel fire with Insufficient Ventilation to Prevent Backlayering; bottom: Tunnel Fire with Sufficient Ventilation to Prevent Backlayering [3]

is only one plenum either supplying or extracting air, in contrast with fully transverse system. In normal mode, fresh air is supplied along tunnel and smoke flows towards the portals and is vented out to atmosphere. In reverse mode, smoke is extracted along the tunnel and fresh air is supplied from the portals [12]. The main advantage of transverse ventilation system is that localised smoke extraction is possible and stratification of smoke layer can be achieved along the full length of tunnel, in principle.

2.3.3 Critical Ventilation Velocity

The critical ventilation velocity (CVV) is defined as the minimum ventilation velocity that eliminates backlayering and the value is the primary criterion when designing longitudinal ventilation system. CVV is proportionate to the fire size (heat release rate), according to various studies [9] [10] and it is affected by several factors such as tunnel slope, vehicular obstruction and tunnel cross sectional area. Several studies have shown

that there is a 'super critical' ventilation velocity above which backlayering does not depend on fire size anymore. Oka and Atkinson [9] have proposed a dimensionless equation after carrying out small scale experiments:

$$\begin{aligned} V_c^* &= K_v(0.12)^{-1/3}(Q^*)^{1/3}, \quad Q^* < 0.12 \\ 8V_c^* &= K_v, \qquad\qquad\qquad\quad Q^* > 0.12 \end{aligned} \tag{2}$$

where

$$Q^* = \frac{Q}{\rho_0 c_p T_0 g^{1/2} H^{5/2}},\ V_c^* = \frac{V_c}{\sqrt{gH}}$$

where V_c^* is the dimensionless critical ventilation velocity, K_v is the experimental constant, Q^* is the dimensionless heat release rate, ρ_0 is the density of air, c_p is the heat capacity of air, T_0 is the ambient temperature, g is the gravitational constant ($9.81 m/s^2$) and H is the tunnel height. Values of K_v vary between 0.22 and 0.38 according to the burner used. This set of equation works for flames lower and higher than tunnel height.

Wu and Bakar [10] also proposed similar equation after carrying out small scale experiments and CFD simulations, describing using tunnel hydraulic diameter instead of the actual height:

$$\begin{aligned} V_c^* &= 0.40(0.12)^{-1/3}(Q^*)^{1/3}, \quad Q^* \leq 0.2 \\ V_c^* &= 0.40, \qquad\qquad\qquad\quad Q^* > 0.20 \end{aligned} \tag{3}$$

where

$$Q^* = \frac{Q}{\rho_0 c_p T_0 g^{1/2} \bar{H}^{5/2}},\ V_c^* = \frac{V_c}{\sqrt{g\bar{H}}} \tag{4}$$

The reason Wu and Bakar used hydraulic diameter, which is defined as 4 times the cross sectional area divide by the perimeter ($\bar{H} = 4A/P$), is because the CVV changed

significantly with different cross sectional area and when hydraulic diameter is used, the experimental results reach a better agreement. In fact, there is a good agreement between the small scale and large scale tests such as the Memorial tunnel tests and the Buxton gallery tests [10].

According to Atkinson and Wu's study [19], there is a relationship between tunnel slope and the CVV, and the formula for correction factor is described as:

$$V(\theta) = V(0) * (1 + 0.014\theta) \tag{5}$$

where θ is the slope in degree and V(0) is the critical ventilation velocity in a flat tunnel. The formula, however, is only valid when θ is between 0° and 10°.

Presence of vehicular obstruction also affects the CVV significantly. Li et al. [11] found that when fire was set under a stationary vehicle, which occupied roughly 20% of tunnel cross sectional area, CVV was reduced by 23%. Oka and Atkinson [9] used a propane gas burner positioned outside a solid obstruction in a small scale tunnel. They found that when a vehicle occupied roughly 12% of cross sectional area, the reduction ratio of CVV was 15% and was 40-45% when a vehicle occupied roughly 32% of the cross sectional area.

A study by Lee and Tsai [20] found that CVV decreases due to vehicular obstruction when ventilation flow reaches the fire and the reduction ratio approximately equals the vehicle blockage ratio by the continuity equation. The experiment in the same study showed that when fires were located at downstream of vehicles, in contrast to Li's study [11], the change ratio of CVV was slightly greater than the tunnel blockage ratio. Lee and Tsai then hypothesised that the decrease in CVV can be estimated as the tunnel blockage ratio adjusted by the effect of the local ventilation flow area, which depends on the relative position of fire source.

A relatively new term 'confinement velocity' has been introduced by Vauquelin and Telle

[21]. The definition of the confinement velocity is the longitudinal velocity induced by extraction which is necessary to prevent the smoke layer development after the last exhaust vent has been activated. It is the lowest velocity needed to prevent existing backlayering at a certain position, i.e. to prevent further spread upstream, while preserving certain stratification. The confinement velocity was then defined when the backlayering distance is lesser than 4 times the tunnel height upstream at the extraction vent.

Results from small scale tests by Li et al. [11] show that the backlayering length and the dimensionless confinement velocity, which is the ratio of longitudinal ventilation velocity to critical velocity, follows an exponential relation:

$$\begin{aligned} V^{**} &= exp(-0.054 l^*) \\ V^{**}_{ctr} &= exp(-0.074 l^*_{tr}) \end{aligned} \tag{6}$$

where V^{**} and V^{**}_{ctr} are the dimensionless confinement velocity without and with vehicular blockage respectively, and l^* and l^*_{tr} are the dimensionless backlayering distance without and with vehicular blockage.

They proposed a piecewise function to express the dimensionless critical velocity in a tunnel with and without vehicular blockage as

$$\begin{aligned} V^*_c &= \begin{cases} 0.81 Q^{*1/3}, & Q^* \leq 0.15 \\ 0.43, & Q^* > 0.15 \end{cases} \\ V^*_{ctr} &= \begin{cases} 0.63 Q^{*1/3}, & Q^* \leq 0.15 \\ 0.33, & Q^* > 0.15 \end{cases} \end{aligned} \tag{7}$$

where V^*_c and V^*_{ctr} is the dimensionless critical velocity without and with vehicular blockage.

They also proposed that the dimensionless backlayering length without obstruction in a

tunnel can be expressed as

$$l^* = \begin{cases} 18.5\ln(0.81Q^{*1/3}/V^*), & Q^* \leq 0.15 \\ 18.5\ln(0.43/V^*), & Q^* > 0.15 \end{cases} \tag{8}$$

where V^* is the dimensionless longitudinal ventilation velocity and Q^* is the dimensionless heat release rate. The relationship fits well with the large-scale tests at Yuanjiang tunnel.

There is currently a lack of research on how the critical ventilation velocity or backlayering length is affected by the height of fire, or when translated to real life situation, the height of vehicles caught on fire.

2.3.4 Fire Throttling Effect

Throttling effect of air occurs when there is excess aerodynamics resistance in the ventilation stream. Fire causes throttling effect by adding heat and mass into the tunnel, creates disturbance to the cold equilibrium operating condition and hence increases the flow resistance inside the tunnel. In serious situation, the disturbance can cause reverse flow of air against ventilation.

The fire throttling effect was first experimentally studied by Lee et. al in 1979 [13]. They compared the gas mass flow rate in the model tunnel network when under cold condition and during fire. Their results showed that the flow resistance in the fire zone was increased by a factor of 6, and upstream and downstream of the fire by around 1.5 times. They stated that throttling became more severe at high air flow rate as higher air flow rates intensified the fire. Their results also showed that the ventilation air can be indirectly throttled by the fan if the gas temperature at the fan is sufficiently high.

Coupling of a physical ventilation system to a fire and quantification of the fire throttling

effect was first done by Colella et al. [22] using multiscale methodology which combines mono-dimensional (1D) and CFD (3D) modelling techniques to model a 1.2 km long tunnel. Various fire sizes ranging from 10 MW to 100 MW were investigated with a varying number of jet fans and their results showed that the flow was reduced up to 30 % for a 100 MW fire.

The impact of change in fire size on tunnel jet fan system was studied by Vaitkevicius et al. [23] using FDS. The study showed that by increasing fire size, the number of jet fans required to prevent backlayering increases, although the critical ventilation velocity does not vary much from the proposed formula by Wu and Baker [10].

It is one of the main objectives of this project is to investigate the throttling effect when a new component, which is the water mist system, is added to the coupling of jet fan system and fire.

2.3.5 Effect of Tunnel Ventilation System on Fire

The presence of tunnel ventilation system has an impact on the fire characteristics. The effect of longitudinal ventilation on the fire HRR has been studied by various researchers. Forced ventilation will affect different types and sizes of fire loads in various ways as it will carry along a handful of oxygen which changes the ventilation factor of the fire and at the same may have cooling effect. It may also change the fire spread rate or even extinguish the fire entirely. The mechanism of burning a pool fire and solid fuel is fundamentally different and therefore forced ventilation will have different impact on different types of fire. For solid fuel, say a vehicle fire, forced ventilation may blow through the fire load, causing the fire to spread and grow in intensity [24]. Pool fire has an entirely different reaction to forced ventilation compared to solid fuel as all the combustion happens at the surface, not inside the load. This project will only focus on vehicle fires, in particular heavy good vehicles (HGV) as HGVs are often considered the highest risk.

A study on the effect of forced ventilation on a HGV fire, which features variation of HRR with ventilation velocities up to 10ms^{-1}, has shown that longitudinal ventilation may cause a fire to spread through a HGV over twenty times faster, and reach a maximum HRR eight or nine times larger, than with natural ventilation [25]. Carvel [24] [25] has introduced a Bayesian method to estimate the factor of HRR enhancement in the presence of forced ventilation by the following formula:

$$Q_{vent} = kQ_{nat} \tag{9}$$

where Q_{vent} is the HRR of a vehicle fire in a tunnel with forced ventilation, Q_{nat} is the HRR of a similar fire with natural ventilation, and k is the heat release rate coefficient. For a HGV fire in the growth phase, he estimated k highly likely to be 8-16 at 2 ms^{-1}, 16-32 at 4, 6 and 8 ms^{-1}. For a HGV fire at maximum heat release rate, he estimated k highly likely to be 4-8 at 2 and 4 ms^{-1}, 8-16 at 4, 6 and 10 ms^{-1} and 16-32 at 10 ms^{-1}. It is therefore concluded that forced ventilation does not have a constant influence over fire over time, and it depends on whether the fire is in the growth phase or steady state.

A model scale tunnel fire test conducted by Ingason and Li [26] shows that, however, the fuel mass loss rate per unit fuel surface area, which is proportionate to HRR, is only a weak function of the ventilation velocity. They explained that the difference with Carvel's estimation is probably due to the way the fuel was compared. The study also confirms that the fire growth rate will increase according to longitudinal ventilation rate. The paper also shows that backlayering length is independent of the HRR for a large tunnel fire.

2.4 Fixed Firefighting System (FFFS)

Fixed firefighting system comes in various forms and extinguishing agents. Till present, despite the latest developments of other suppression agents, water is still the primary choice for a couple of reasons. Firstly, in terms of mass, fine water mist droplets are at least as effective as Halon 1301 (CF_3Br) due to its large latent heat of evaporation and

heat capacity of water vapour. It takes 335 KJ of energy to heat 1L of water from 20 to 100°C and 2257kJ to turn into steam. Secondly, water has very little health and environmental impact, which is critical in tunnels where the extinguishing agent is exposed to human contact as well as the atmosphere. Lastly, water is also the most cost effective agent, which makes it suitable to cover the large floor area in any tunnel.

It is recognised by the World Road Association (PIARC) and the National Fire Protection Association (NFPA) that active fire protection systems can limit the size and growth of a fire, prevent the fire from spreading and improve conditions for first responders. It could also protect tunnel lining, possibly reducing the amount of passive structural fire protection and making significant construction and operation savings. NFPA 502 was also concerned with the reliability of fire detection technology, further visibility reduction and the impact of the FFSS on the effectiveness of tunnel ventilation.

NFPA 502 [3] has then categorised FFFS into four categories based on their performance objectives:

- Fire suppression system: To greatly reduce the heat release rate of a fire and prevent its growth.
- Fire control system: To limit the size of a fire by decreasing the heat release rate and pre-wet adjacent combustibles.
- Volume cooling system: To provide substantial cooling of product of combustion.
- Surface cooling system: To provide direct cooling of critical objects without directly affecting heat release rate.

PIARC historically has been conservative and careful with the recommendation of using FFFS. Their main concerns about FFFS are:

- An FFFS may cause an explosion in the tunnel while suppression of Class B fires (liquid or liquefied solid fires).

- An FFFS may lead to steam injuries to the evacuating people.
- In a vehicle fire, the FFFS cannot suppress the fire from the inside of the vehicle.
- The FFFS activation may lead to the de-stratification of smoke in a tunnel fire.
- Installation, maintenance, and repair cost of the FFFS may exceed the possible annual economic loss in a tunnel fire.
- There might be a possibility of a malfunctioning or false activation of the FFFS.

The main types of FFFS implemented in tunnel fire safety design are sprinkler systems, water deluge systems and water mist systems. The latter two are preferred over traditional automatic sprinkler systems used in buildings due to a few reasons. These two systems are activated by open nozzles instead of localised fire detection, which allow tunnel operators to decide the areas to focus on, instead of activating FFFS over the whole tunnel following the smoke spread. This directly avoids the need of huge water supply, which is important for tunnels at rural areas and prevents excessive water damage. Activation by open nozzles rather than localised fire detection also gives flexibility to the tunnel operators as the system should only be activated after occupants have safely evacuated from incident tunnel as water will dilute and destroy the stratification of smoke layer, reducing visibility in certain areas and introducing more toxic gas to occupants.

FFFS can be categorised into high, medium and low pressure system based on the minimum operating pressure [4]:

Table 2.1: Working Pressure Classification

Minimum Working Pressure	Type of System
$>$ 60 bar	High Pressure System
16 - 60 bar	Medium Pressure System
$<$ 16 bar	Low Pressure System

FFFS is currently not mandated in most countries, only Japan and Australia has adequate experience using the technology and more countries are exploring the feasibility

of protecting their tunnels using FFFS. In Australia, water deluge systems are installed in all major urban road tunnels, including Sydney Harbour Tunnel, M4 Tunnel and City Link Tunnel. In Japan, FFFS are required to be installed in all tunnels longer than 10,000 m and in tunnels longer than 3000 m with heavy traffic. A number of European countries including Austria, France, Italy, Norway, Netherlands, Spain, Sweden and United Kingdom have installed FFFS in tunnels. Only six road tunnels are currently equipped with FFFS in North America [3].

2.4.1 General Guidelines of Fixed Fire Fighting System

NFPA 502: Standard for Road Tunnels, Bridges, and Other Limited Access Highways [3] and *Engineering Guidance for Water Based Fire Fighting Systems for the Protection of Tunnels and Subsurface Facilities* [4] provide general guidance on the arrangement of FFFS, without prescriptive values. It is recommended that proper engineering analysis is performed for different tunnels. The setup of simulation in this project shall follow most of the suggestions given in these guidelines if possible, in order to make the simulation realistic and applicable to real life design.

Engineering Guidance for Water Based Fire Fighting Systems for the Protection of Tunnels and Subsurface Facilities [4], which was written alongside the European Research Project UPTUN, provides a few suggestions for FFFS design:

- Fire fighting nozzles are normally installed under the ceiling or the upper part of the side walls, pointing downwards or at the centre of the tunnel.
- The whole tunnel should be covered with nozzles, which are grouped into sections. The section length shall be defined on case by case basis and engineering analysis and shall not be shorter than 30m.
- All sections are connected by section valves and a main water supply line to the pump unit. In order to ensure sufficient water supply, the water supply line should be able to provide water at the minimum pressure for at least two sections simultaneously.

- To ensure effective and efficient fire suppression, a group of nozzles forming a section shall be activated simultaneously in the upstream and downstream of the fire.

NFPA 502 suggests that for an active fire protection system to be effective, the followings are recommended:

- FFFS can be designed as a manually activated deluge system with an automatic release after a time delay which should not exceed 3 minutes.
- The piping should be arranged using interval zoning to focus on discharging on the area of incident.
- Nozzles should provide an open deluge and the system should have enough water capacity to allow operation of at least two zones in the incident area. The zone length should be based on vehicle length, hydraulic analysis and be coordinated with detection and ventilation zones.
- A full-time attended control room should be available for system control and activation.

Both standards do not provide any methods to determine the activation sequence or time.

2.4.2 Dynamics of Fire Suppression by Water Sprays

Fire suppression by water is mainly due to the gas phase cooling, fuel cooling, displacement of oxidant and the attenuation of thermal radiation.

Gas phase cooling, also known as heat extraction, is a process of lowering the ambient temperature by turning the water mist from liquid phase to gas phase. Water is effective in gas phase cooling owing to its large latent heat (2270kJ/kg) and high specific heat of water vapour. For solid fuel and liquid pool fires, volatilisation of fuel can be reduced

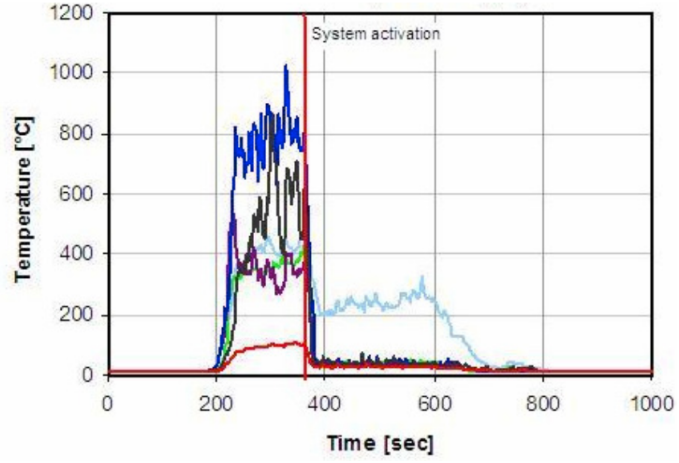

Figure 2.4: Gas Phase Cooling Effect during UPTUN Fire Test [4]

as this process reduces the feedback of heat from the fire. The gas phase cooling effect can be demonstrated from the full scale test result from the European research project UPTUN, as shown in Fig. 2.4, which shows the drastic decrease in gas temperature after water mist .

Fuel cooling, as known as direct cooling, occurs when water droplets reach the fuel surface directly. Fuel volatilisation rate is reduced and fire spread can be prevented as a result. Effectiveness of fuel cooling by water droplets is related to its diameter - small droplets such as those in water mist systems evaporate faster and have lower terminal velocities, thus will not penetrate as far as larger droplets [16].

Since water evaporates almost 1,700 times during the process of evaporating, it occupies the place of initial oxidant, which in most cases oxygen. It in turn disrupts the entrainment of oxygen into the flame. Once the oxygen concentration level is below the limiting oxygen concentration, combustion will stop and flame can be extinguished. This phenomena is also known as oxygen displacement. Study shows that effectiveness of water mist on oxygen displacement is augmented in enclosures [27].

In attenuation of thermal radiation, when droplet enters the space between flame and the surface of fuel, it could reduce the evaporation of fuel as well as combustion as feedback

of heat is reduced. However according to Jiang et al. [28], radiation attenuation is seldom sufficient to extinguish a fire, as water absorbs radiation only at certain wavelengths.

2.4.3 Water Mist System

According to NFPA 750 and NBN CEN/TS 14972 standards, a water mist is a spray consisting of droplets with a characteristics diameter $D_{V0.9}$ less than 1mm, meaning that at least 90% of the total water volume are smaller than 1mm. NFPA 750 further classifies water mist into 3 classes, as summarised in Table 2.2.

Table 2.2: Water mist system classification according to NFPA 750

Class I	Class II	Class III
$D_{V0.9} \leq 200\mu m$	$200\mu m \leq D_{V0.9} \leq 400\mu m$	$400\mu m \leq D_{V0.9} \leq 1000\mu m$

The choice of water mist class is similar to the comparison between water mist and water deluge system. Class III water mists according to Table 2.2 are better for Class A fires (solid fires) as the larger droplets have higher terminal velocity and thus higher probability to reach the fuel seat, in order to cool down the solid fire or even extinguish it. Class I mists are more efficient for gas phase cooling than other two classes as smaller droplets have larger surface-to-volume ratio [8]. In tunnel fires the fire is often shielded or hidden by vehicle roof, which makes fuel cooling nearly impossible. Therefore Class I water mist is more suitable in such cases.

A study by Wang [29] shows that the optimal droplet size for water mist for the best suppression effectiveness is in the range between 50 μm and 300 μm and he recommended using 60 μm at the flow rate of 5 L/min based on the compromise between extinguishing time and water consumption. There are a few reasons why smaller droplet sizes are more effective at suppressing fire. Firstly, because of lesser weight, the droplets have lower momentum when ejected from the nozzle and therefore have more time to absorb surrounding heat before hitting the ground. Secondly, smaller droplet diameter will result in larger quantity of droplets given the same flow rate and combined with its larger surface area to volume ratio, smaller droplets are better at oxygen displacement

than larger droplets. According to Wang's study, the radiation absorbed by water mist is nearly the same for 100 μm and 1000 μm droplet, and the medium droplet sizes perform poorly in extracting radiation.

Water mist systems, by their very nature, are unable to suppress large fires as the water droplets are so fine that they are most likely to evaporate in the fire plume region before reaching the fuel bed to suppress the fire. Numerous researches have been conducted to study the effectiveness of WMS on fire including tests conducted in tunnels and in enclosures. Meeussen et al. [30] concluded that WMS can extinguish or control a 200 MW liquid fire fast enough to prevent a boiling liquid expanding vapour explosion (BLEVE), water mist system can reduce and control a 50 MW solid fire and in the case of 200 MW solid fire, the limits of water mist system were approached.

A reduced scale experiment study done by Sun et al. [31] has shown that in a naturally ventilated tunnel, when water mist system is installed a distance away from fire, smoke is blocked by the water system. Whereas under longitudinal ventilation, smoke is no longer blocked by the water system.

The experiment result from Project SOLIT (Safety of Life in Tunnels) conducted in 2006 in the Spanish test tunnel of TST (Tunnel Safety Testing) shows that if the water mist system is activated in time, the fire size of a truck-simulating fire load can be limited to below 60 MW compared to 120 MW without activation. The experiment has also stated that by activating a fire-extinguishing system, visibility is ensured completely on the upstream as there is no backlayering observed as a result of interaction of water mist system and ventilation [15].

An experimental study done in tunnels by Chen et al. [32] shows that fire suppression process using water mist has three stages: (1) Flame unitary restraining stage, (2) surface flame extinguishing stage and (3) inside flame suppression stage. The paper also explored the influence of longitudinal ventilation velocity to the performance of water

mist suppression system. It states that when the fuel load is located directly below the nozzle, suppression time will be prolonged along with the increase of ventilation velocity. Different intervals between nozzle and fuel load will also have different optimum ventilation velocities for minimum fire suppression time. Furthermore, when the ventilation velocity is too high, flame will be depressed excessively by airflow, lowering the flame height. Combining with the fact that mists will move rapidly with the airflow, fire extinguishing time will be extended as lesser mist reaches on the flame surface. Similar experimental study by Zhang et. al [33] to study interaction between fire and water mist in long and narrow spaces shows that, nozzle operating pressure of 20 bar and 30 bar water mist intensified the fire. With 40 bar, restraining effect has improved; at 60 bar, flashover was effectively suppressed and finally at 70 bar, water mist successfully suppressed the fire.

Manufacturers recommend that water mist system to be operated over a length of 100 to 150 m, comprises of two or three sections, such that the sections are only limited to areas where smoke temperature is high enough to vaporise the droplets, with the consideration of uncertainty of fire location [8].

2.4.4 Effect of Longitudinal Ventilation on Water Mist System

The effect of longitudinal ventilation on the water droplets used in WMS is certainly non-negligible due to their small mass. There are several researches focusing on the interaction between water mist system and tunnel ventilation system.

Crosfield et al. [34] has previously conducted small scale experiment and CFD modelling to determine the landing distance of droplets under the influence of longitudinal ventilation. It was found that most water mist droplets, with diameter lesser than 170 μm, are carried between 60 and 130 m downstream before they hit the ground, under 3 ms^{-1} of ventilation velocity. Under flow of 10 ms^{-1}, the droplets are carried between 130 and 750 m downstream. According to Maevski and Klein [18], when the water mist

system is activated in conjunction with the longitudinal ventilation system, nozzles at upstream and midstream of smoke should be activated to take the blow-away effect into account.

On the other hand, the presence of WMS is expected to influence the ventilation system as well, due to the drag caused by water droplets when ventilation flow passes through them. The drag force is either expressed by the drag equation for high velocity flow, non viscous fluid $F_D = 0.5\rho v^2 C_d A$, or by the Stoke's Law $F_D = -bv$ for viscous fluid, where ρ is the density of fluid, v is the speed of object relative to the fluid, C_d is the drag coefficient and A is the cross sectional area of the object. However there is no study exploring the effect to date.

Wu and Hsu [35] has analysed the effects of critical velocity with water deluge system with droplet sizes ranging from 800 to 1200 μm. Their result shows that the critical velocity is lower after using the water spray system. Critical velocity is also lower when smaller droplets are used. Their finding suggests that the more cooling the water spray system can achieve, the lower the critical velocity. It is one of the main objectives in this project to investigate if similar conclusion can be made when simulating using jet fan, instead of a fixed velocity vent boundary and using water mist, instead of water deluge.

3 Fire Dynamics Simulator (FDS) Modelling Input Parameters, Assumptions and Limitations

3.1 Introduction

FDS version 6.5.3 is used for this project. FDS is a CFD model of fire-driven fluid flow [5], first released in February 2000 by National Institute of Standards and Technology (NIST) as a free and open-source software. It is a large-eddy simulation (LES) code. There are three key components in the model:

- Hydrodynamic Model: FDS solves numerically a form of Navier-Stokes equations for low-speed flows (Ma < 0.3), thermally-driven flow emphasising on smoke and heat transport from fires, with an explicit predictor-corrector scheme, second order accurate in space and time core algorithm. Turbulence is treated by means of LES by default or Direct Numerical Simulation (DNS) if the mesh is fine enough. User can choose either Deardorff (default), Dynamic Smagorinsky, or Vreman as the turbulence model.
- Combustion Model: FDS mostly uses a single step, mixing-controlled chemical reaction using three lumped species, which are air, fuel and products. The latter two are explicitly computed by default.
- Radiation Transport: Radiative heat transfer is computed largely via the solution of the radiation transport equation for a gray gas, and in some case via a wide band model. The radiation transport equation is solved using Finite Volume Method (FVM).

FDS is often paired with Smokeview, which is another freeware by NIST as a visualisation tool specifically for FDS. Smokeview is capable of producing slice files for measured quantities in FDS such as temperature, velocity, mass fraction, 3D smoke file which is useful to visualise how smoke develops and particle file to show the particle movement injected into the model, such as water droplets from nozzles.

3.2 Software Validation

FDS has long been used and validated by many researches to model tunnel fire, tunnel ventilation system and water mist system.

3.2.1 Tunnel Fire and Ventilation System

Hwang and Edwards [36] used FDS Version 2 to model the critical ventilation velocity in a ventilated tunnel and verified the results with the experimental data obtained at the Memorial tunnel (large tunnel) and by Hwang and Wargo (small tunnel) [37]. Ventilation flow was generated by assigning a volumetric flow rate at the tunnel inlet and atmospheric pressure at the outlet, which is a common approach in CFD tunnel fire simulations. Their results showed that the leveling-off of CVV as the fire heat generation increases, that the fuel type and ambient temperature have negligible effects on the value of CVV and that FDS is capable of predicting the CVV with various size and configuration.

Kim et al. [38] have carried out simulations using FDS Version 4.0 to simulate a fire in a tunnel using a gas burner with approximately 100MW of HRR, in order to predict the temperature profile and backlayering of a pool fire in the tunnel with appropriate grid size and boundary conditions. They also evaluated the Smagorinsky constant, turbulent Prandtl number and the Schmidt number in the model. They concluded that FDS shows its limitation in predicting the smoke layer near the ceiling at the upstream region of the tunnel.

Bilson et al. [39] used FDS to study the interaction of a deluge system with a tunnel ventilation and smoke exhaust system.

Li and Ingason [40] simulated the Runehammer Tunnel T1 test, where an HGV mock-up was used, using a gas burner with specified HRR inputs. They found that the ceiling gas

temperature corresponded well with the experiment results on the downstream of fire from 10 to 150 m. However the temperatures for further downstream (250m, 350m and 450m) were overestimated. Besides that, the incident heat fluxes at the downstream of fire from the simulation did not match well with experiment results.

3.2.2 Water Mist System

Kim and Ryou [41] compared FDS predictions to results of compartment fire test with and without the application of a water mist. FDS gave good prediction in the gas temperature and oxygen dilution as the results were within about 10% of measurements. However, the simulations failed to predict the complete extinguishment of a hexane pool fire. They attributed that to be the result of combustion model rather than the droplet model.

Hostikka and McGrattan [42] investigated the thermal radiation absorption by water sprays in FDS and concluded that FDS is able to predict the radiation attenuation when the hydrodynamic interaction between the droplets is weak.

FDS Version 6.5.3 uses a new droplet evaporation scheme using implicit approach developed by Floyd and McDermott [43], which solves the problems of droplets impacting hot surfaces with low conductivity and low thermal inertia and simulations with very fine water mist in the older versions. The new evaporation scheme was validated and verified through a series of tests.

3.3 Geometry

Only single bore tunnel will be studied, as this project only focuses on longitudinal ventilation system which is mostly used in single bore unidirectional tunnels. The tunnel is modelled as a 6 m x 6 m square and 600m long. The reason for the length is that a flat tunnel is generally considered long if its length exceeds 600 m [44] and beyond this length stable stratification will not sustain for natural ventilation [45], thus longitudinal

ventilation system is mandatory. The width and height of the tunnel is chosen arbitrarily to represent a tunnel which allows heavy good vehicles to enter.

The surface of obstructions in the FDS model is all set to be inert, which means the temperature of tunnel walls is fixed at the ambient temperature, which is 20°C in this model. This assumption is deemed suitable as the tunnel walls are normally physically and thermally very thick and likely to have negligible temperature change when exposed to fire. Additionally the simulation time can be reduced significantly by neglecting the surface material property.

3.4 Design Fire

The design fire size ranges from 20MW to 60MW, with 10 MW step increment for different scenarios and 40MW as the base case scenario, to represent a HGV fire, as described in Section 2.2 and it is modelled with a prescribed heat releaser rate per unit area (HRRPUA) in FDS. The dimension of the HGV and fire surface is shown in Fig. 3.1. The height of the fire surface on the side is only 1 m tall so that the height of the HGV can be altered for different fire scenarios, which will be discussed in Section 3.10.2, while keeping the HRRPUA as constant.

As the HRR output is always constant, this project does not take either the change in fire size or pyrolysis rate due to FFFS or tunnel ventilation system or fire extinction that was mentioned in previous sections into consideration. Instead, it is intended for readers to use the value they wish to study after calculating the effects of various components on fire, due to the complexity of the problem. Only a single vehicle is simulated, therefore fire spread is not studied in this project.

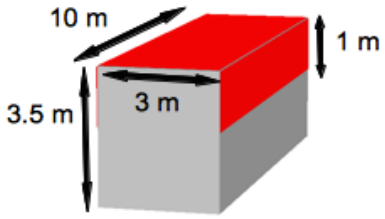

Figure 3.1: Dimension of the HGV obstruction and fire surface

3.5 Jet Fans System

Instead of imposing boundary condition of certain velocity or pressure at the tunnel portals like many studies have done so [10] [46] in order to directly determine the critical ventilation velocity, this project aims to accurately simulate longitudinal ventilation system in a tunnel, which normally features jet fans. The simulation models jet fans according to suggestions from the Sixth Edition FDS User Guide [5]. The jet fans are modelled as a heating, ventilation, and air conditioning (HVAC) system with an inlet and an outlet vent attached to a solid obstruction to represent the physical space a jet fan occupies. Under such configuration, due to the assigned pressure difference by FDS, air will be sucked into the inlet vent, transported through the model HVAC system and exhausted from the outlet vent towards the fire. The advantage of using HVAC method to model jet fans is that it allows hot, smoky gases to pass through the obstruction.

FDS allows user to specify many input parameters to accurately model the air flow. In this project, the diameter and the volume flow rate of the jet fan is specified and FDS will calculate the outflow velocity by dividing the volume flow rate by the cross sectional area, which is determined by the diameter specified. The jet fans chosen for this project are tunnel jet fans manufactured by POLLRICH GmbH [47]. The model chosen is consistent for every fire scenarios for fair comparison, and the summary is provided in Table 3.1.

Table 3.1: Jet Fan Model Used

Parameter	Value
Jet Fan Model	SATM-0900-B
Diameter (mm)	840
Volume Flow Rate (m^3/s)	16.9
Total Length (mm)	3075
Downward Shroud Length (mm)	1200

3.5.1 Jet Fan Shroud

Additionally, according to a validation study by Thunderhead Engineering [48], FDS models jet fans more closely matched to experimental data when downstream shroud is included, and the mesh size of Diameter/2 performs quite well in matching the centerline velocity decay and the flow entrainment. This is because the downstream shroud makes sure the outlet flow is in the axial direction and not expand in the first cell downstream of the vent. Therefore in this project the shroud of jet fan is modelled using the dimension in the manufacturer brochure, as shown in Fig. 3.2, and the mesh size around the jet fan is 1 m/2 = 0.5 m. A comparison of how the shroud affects the flow pattern in this model is shown in Fig. 3.3. As seen in the figure, with downstream shroud, the jet fan flow travelled at least 25 m longer than the other model and represents a real jet fan flow better.

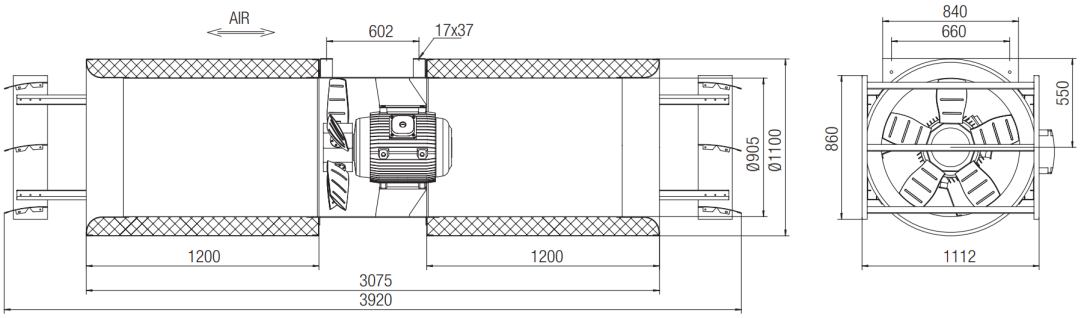

Figure 3.2: Dimensions of the jet fan modelled

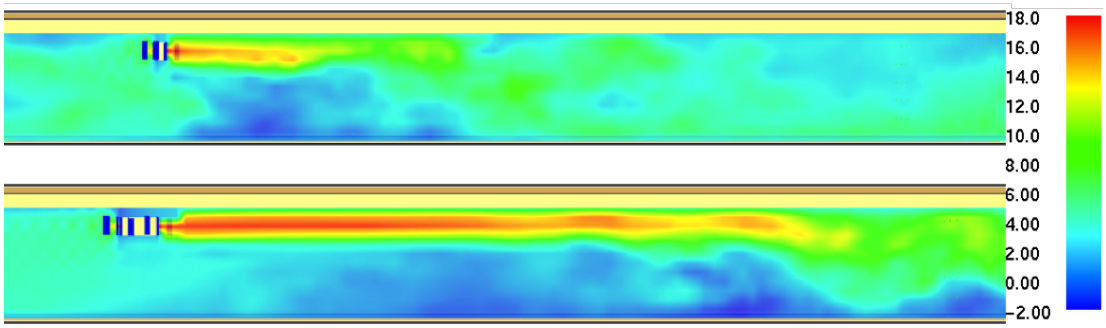

Figure 3.3: Longitudinal velocity slice file on the scale of -2.0 to 18.0 m/s. Top: FDS simulation without downstream shroud; bottom: FDS simulation with 1 m long downstream shroud

3.5.2 Jet Fan Location

There are three rows of three jet fans modelled, considering the tunnel geometry. The jet fans at the same row are 0.5 m away from the wall, 1 m away from the adjacent jet fan and 0.5m away from the ceiling, and the cross-section arrangement and dimensions are shown in Fig. 3.4. Each row of jet fans is 50 m apart from the next row and placed near a tunnel portal, similar to the multi-scale model by Colella et al. [14]. Configuring fans such that blowing air from upstream of the fire is more effective in minimising fire throttling effect, which occurs if the gas temperature at the fans is sufficiently high [13]. The closest row of jet fans to the fire location is 50 m. This close distance is chosen because this project intends to study how smoke, ventilation system and water mist system affect each other at shorter distance, which is deemed challenging for jet fans to manage tunnel air velocities during fire [44]. The plan view of the tunnel is shown in Fig. 3.5.

3.5.3 Fan Activation

The usage of fans follows the numbering in Fig. 3.5. For example, if the result shows that two jet fans were needed, it means that jet fan number 1 and 2 were activated; if four jet fans were needed, jet fan number 1, 2, 3 and 4 were activated, and so forth. The activation of jet fan is achieved using the RAMP function in FDS and the time between activation of each fan is five minutes in order for the flow to reach steady state for a

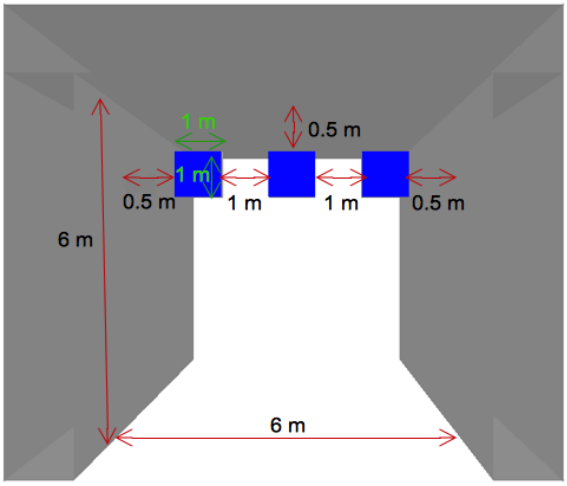

Figure 3.4: Cross Section View of Jet Fans

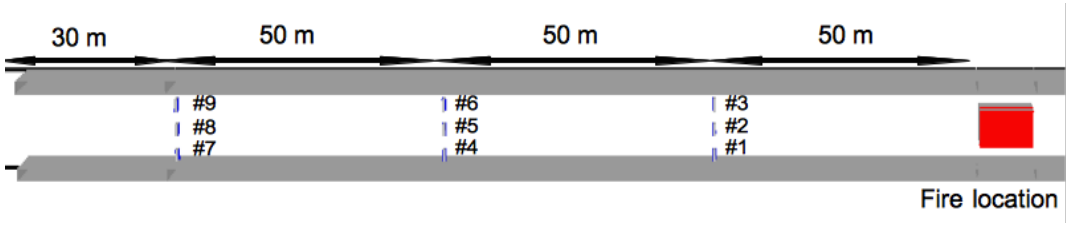

Figure 3.5: Plan View of Jet Fans and Fire

considerable amount of time. The five minute interval is determined by velocity over time graph measured, as described in Section 3.9, as it takes around three minutes for the longitudinal velocity to be steady and two more minutes so that the fluctuation of value can be more averaged out.

3.6 Water Mist System

Eulerian-Lagrangian approach is used in FDS to treat the gas phase as a continuum and the water droplets as individual dispersed Lagrangian particles. This method is used because the water droplets are too small for the computational mesh to resolve. The Eulerian equations, governing gas and droplet thermal-hydraulic behaviour, droplet and flame interaction and fire suppression characteristics, include the continuity, momentum, energy and state equations. The Lagrangian equations consist of position, mass, momentum and energy [5].

The momentum transfer from the Lagrangian particles to the Eulerian equations is via the body force term f_b in the Navier-Stokes momentum equations [49]:

$$\rho(\frac{\partial \mathbf{u}}{\partial t}) + (\mathbf{u} \cdot \nabla)\mathbf{u}) + \nabla p = \rho \mathbf{g} + \mathbf{f}_b + \nabla \cdot \tau_{ij} \tag{10}$$

where ρ is the density of fluid, $\mathbf{u}$ is the fluid velocity in 3D, p is the pressure of flow field, $\mathbf{g}$ is the gravitational constant, f_b is the body force exerted on the fluid, and τ_{ij} is the stress tensor.

$\mathbf{f}_b$ is calculated by summing the force transferred from each particle in a grid cell and divide by cell volume, V:

$$\mathbf{f}_b = \frac{1}{V} \sum [\frac{\rho}{2} C_d A_{p,c} (\mathbf{u_p} - \mathbf{u}) |\mathbf{u_p} - \mathbf{u}| - \frac{dm_p}{dt} (\mathbf{u_p} - \mathbf{u})] \tag{11}$$

where ρ is the fluid density, C_d is the drag coefficient, $A_{p,c}$ is the particle cross-section area, $\mathbf{u_p}$ is the particle velocity, $\mathbf{u}$ is the fluid velocity, m_p is the particle mass. As shown in Eq. 11, if the first term on the right hand side is larger than the latter term, the body force will have positive value and momentum is transferred from the particles to fluid, vice versa.

The drag coefficient C_d is a function of local Reynolds number that is based on particle diameter, D:

$$C_d = \begin{cases} 24/Re_D & Re_D < 1 \\ 24(0.85 + 0.15 Re_D^{0.687})/Re_D & 1 < Re_D < 1000 \\ 0.44 & 1000 < Re_D \end{cases} \tag{12}$$

$$Re_D = \frac{\rho |\mathbf{u}_p - \mathbf{u}| D}{\mu(T)} \tag{13}$$

where $\mu(T)$ is the dynamic viscosity of air at temperature T. It is difficult to determine the Reynolds number in this model as the velocity of particles varies according to their location and the flow velocity also varies at different height of the tunnel. However it is estimated to be in the region of $1 < Re_D < 1000$.

Correction has to be made to the drag coefficient when the distance among particles is small enough that the individual particles influence each other and cause drag reduction on the particles trailing behind. Drag reduction is expected for water mist droplets as the spray is very dense. However FDS does not specifically calculate the interaction among particles since the separation length is too small for normal grids, and each particle interacts with the fluid individually. Instead, FDS calculates the reduction of the drag on the second particle by:

$$C_d = C_{d,0}\frac{F}{F_0} \tag{14}$$

where $C_{d,0}$ is the drag coefficient in the absence of other particles, and F / F_0 is the hydrodynamic force ratio of the trailing particle to an isolated particle, which will not be explained further in this project. This correlation, however, is deemed to under-estimate the drag reduction significantly at small separation distance, according to Prahl et al [50].

Particles can be initialised to a part of the computational domain at the beginning of a calculation or can be introduced to the flow field from vent surfaces [51]. For a water nozzle, this point is the virtual origin of all particle trajectories and droplets are injected into the field at a spherical surface surrounding the nozzle with radius defined by user.

In practice, it is very difficult to determine the distribution of droplet size due to the lack of data measurement. In FDS, the size distribution of liquid droplets is specified using a cumulative volume fraction (CVF) and the default CVF is 'ROSIN-RAMMLER-LOGNORMAL' [5], as shown in Fig. 3.6. The median volumetric diameter can also be

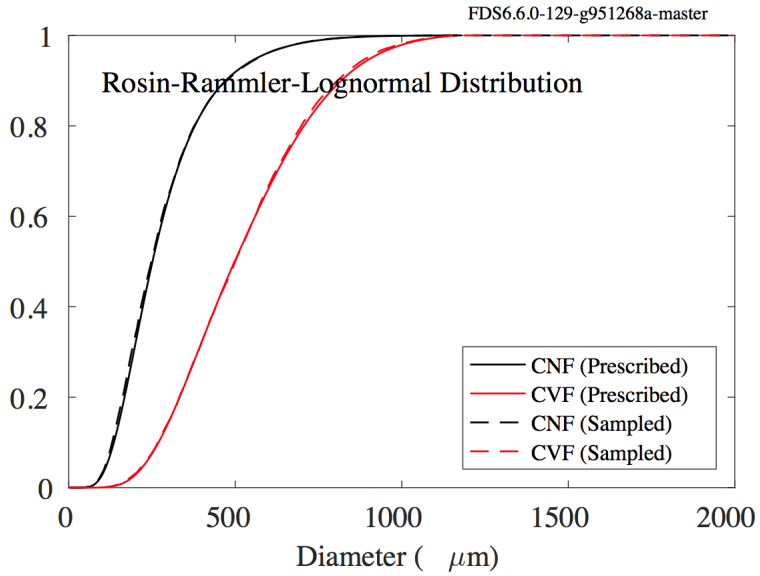

Figure 3.6: Droplet size distribution based on Rosin-Rammler-Lognormal Distribution [5]

specified. The median diameter is chosen to be 200 μm, as it is the largest diameter for Class I water mist system ($D \leq 200\mu m$) which is more suitable for tunnel fires as recommend by CETU [8]. Also the larger the particles are, the lesser computational time needed for the simulation to complete as there are lesser number of particles to compute.

The water flow rate is determined by the system's K-factor K $(l/min/bar^{1/2})$ and operating pressure p (bar) using $Q = K\sqrt{p}$. The K-factor is taken as 4.3 as reference from the study done by Vaari et al. [51] and operating pressure is taken as 40 bar as it is the pressure at which fire straining effect was obvious, according to Zhang et al. [33]. A study by Blanchard et al. [52] suggests that initial droplet velocity at the injection point is not an influent parameter and it has been arbitrarily set to 15 m/s.

The absorption and scattering of thermal radiation by Lagrangian particles is included in the radiation transport equation in FDS, which means the effect of attenuation of thermal radiation by water droplets can be modelled [5]. This project does not attempt to model fire suppression by water mist system, although it has been experimentally proven effective to restrain and suppress flame if the pressure is high enough. However it has been studied numerously that FDS predicts cooling of gas temperature quite well

[51] [41].

Water mist nozzles are placed 0.5 m below the ceiling, which is 5.5 m above floor and discharge water downwards, as suggested in the *Engineering Guidance for Water Based Fire Fighting Systems for the Protection of Tunnels and Subsurface Facilities* [4]. The location and spacing of the nozzles depend on the fire scenarios, as the relative position of nozzles to fire location is one of the factors being studied in this project.

The details of the water mist system modelled in this project are summarised in Table 3.2.

Table 3.2: Characteristics of Water Mist System Modelled

Parameter	Value
K-Factor ($l/min/bar^{1/2}$	4.3
Droplet Size (μm)	200
Nozzle Spacing (m)	Depending on fire scenario, refer to Section 3.10.2
Operating Pressure (bar)	40
Flow rate (l/min)	27.2
Particle velocity (m/s)	15

3.7 Grid Resolution

In order to obtain acceptable and desirable computational result, the cell size of computational mesh should be properly refined in accordance to the appropriate range. As FDS is a LES turbulence model, the more refined a mesh is, the more accurately the model can represent the turbulence, at the cost of extra computational time. This accuracy is particularly important around the region of fire plume as large amount of air is entrained around that area. Striking a balance between grid resolution and computational cost is therefore utmost important when constructing a FDS simulation.

The FDS User Guide [5] suggests the users to calculate the optimal mesh cell size by determining the characteristic fire diameter and cell size ratio based on the total heat

release rate. The following equation shows how the characteristic fire diameter is calculated:

$$D^* = (\frac{\dot{Q}}{\rho_\infty c_p T_\infty \sqrt{g}})^{\frac{2}{5}} \tag{15}$$

D^*/dx ratio should be between 4 and 16 to accurately resolve fires in various scenarios. When $D^*/dx = 4$, the cell size is deemed as coarse, $D^*/dx = 10$ as moderate and $D^*/dx = 16$ as fine. In this project, the areas near fire and water mist nozzles use fine cells, areas adjacent to the fine meshes use moderate cells and other areas use coarse cells. Areas near the jet fans use cell size of 0.5 m, as explained in Section 3.5. Table 3.3 lists the suggested cell size for different HRR.

Table 3.3: Suggested Cell Size for Different Fire Size

Size	20 MW	40 MW	60MW
Coarse	79 cm	105 cm	123 cm
Moderate	32 cm	42 cm	49 cm
Fine	20 cm	26 cm	31 cm

As seen from Table 3.3, the difference of cell sizes between all three fire sizes is not significant, and the cell sizes are decided to be 25 cm, 50 cm and 100 cm for fine, moderate and coarse mesh respectively, regardless of the fire size. An example of the cell size for different meshes is shown in Fig. 3.7.

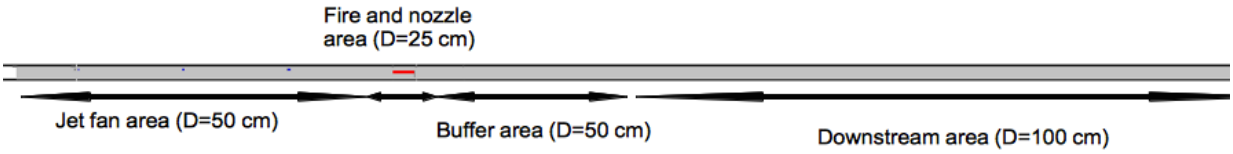

Figure 3.7: Cell Size for Different Meshes

3.8 Time Factor

This project does not attempt to provide any transient solution, such as growing fire rate, linearly ramping up fan capacity or delay activation of component, as the actual

relationship between fire growth rate, ventilation system activation, FFFS detection and occupant self rescue time is too complicated for this project. Several studies have been focused on the time factor on individual components, yet no consensus among the experts towards a standard design procedure has been reached to date. This thesis, rather, provides a steady state solution by changing one variable at a time and allowing the simulation time to develop towards steady state. The results are then collected, analysed and put together for comparison.

3.9 Model Output

In order to determine if backlayering happens, both soot concentration measurement devices and SMOKE3D file are used. There are a few ways to determine if backlayering occurs, such as placing devices at the upstream near the fire location to measure the temperature, velocity or soot concentration at the location of device. Soot concentration is chosen to be determining factor, as the presence of soot directly means that smoke has spread to the location. Temperature is not a suitable parameter as the device will receive radiative heat transfer from the plume and not result in steep temperature change when there is no smoke. Velocity is also not suitable as it is impossible to determine if the flow is ambient air or smoke, in case of getting results in only positive longitudinal direction.

The soot concentration measurement devices are placed in all three directions. They are placed across the tunnel cross section at the upstream of fire location, with 1 m interval across longitudinal and transverse direction and 0.5 m interval from the ceiling. Therefore there are 5 x 5 x 3 = 75 devices at 1 m away from the fire location and every device has to measure below the acceptance criteria for backlayering to be considered not occurring. This acceptance criteria means that it is acceptable for smoke to curl back as long as it does not extend beyond the plane of left side of fire location.

Smoke3D file is an output file created by FDS and rendered by Smokeview to realistically represent smoke and fire, and it is a powerful tool to visually help to confirm

if backlayering occurs and how smoke spreads around the tunnel. The criteria of soot mass fraction for no backlayering happening is set to be below 1 x 10^{-6} kg/kg, which was tested to be the mass fraction below which no backlayering was seen in the Smoke3D file.

Flow measurement devices which measure velocity in longitudinal direction (U-velocity) are placed across the cross section of the tunnel 10 m upstream of fire location in order to measure the flow pattern at every 1 m of height across the location. This will help to understand how the jet fans affect the flow pattern near the fire quantitatively. As there are 6 devices at every 1 m of height, the U-velocity for every height is determined by averaging the measurement values over all 6 devices.

The location and interval of the devices are shown in Fig. 3.8.

In addition to soot and flow measurement devices, water vapour that evaporates from nozzles is also measured following the method mentioned in Section 12.1.5 of FDS User Guide [5] to compare how much water has evaporated with various configurations of water nozzles. Instead of measuring mass fraction as suggested in the FDS User Guide, volume integral of water vapour density across the entire tunnel is measured in order to express the amount of water vapour in smoke layer in terms of mass. As both ends of the tunnel is open, once the flow reaches steady state, the total mass of water vapour will be a steady number when the outflow of water vapour is equal to the water vapour created.

Temperature of smoke layer is not measured using devices in this project, as it is difficult to select suitable locations to place the devices for all scenarios. Under different ventilation condition and other variables, the smoke layer characteristics will be very difficult across different scenarios. Instead, temperature slice files across the entire tunnel are used to provide visual comparison. The redder the slice file is, the higher the gas temperature is. Longitudinal velocity slice files are also useful in understanding the flow pattern visually.

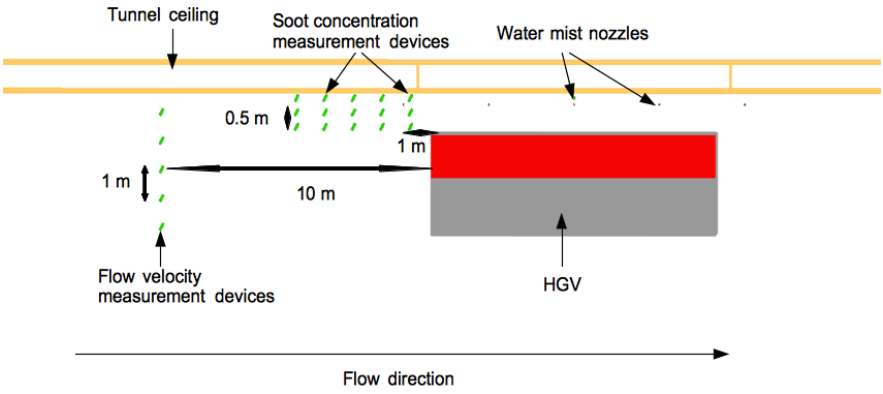

Figure 3.8: Location and Interval of Devices from Section View

In the Result and Discussion Section (Section 4), unless stated otherwise, the number of jet fan, vertical velocity distribution and water vapour mass is all measured after backlayering is prevented.

3.10 Simulation Scenarios

There are three parts of scenarios to be simulated in order to analyse the issue comprehensively and systematically. The first part is a set of test scenarios in which one or two components (out of ventilation system, fire and water mist system) of the model will be absent, so that the effect of individual components can be separated. The second part is the main cases where all three components are put together, with varying parameters to determine how each parameter affects the whole system. The parameters that are varied are the number of water mist nozzles, height of HGV, fire size, water droplet size, location of nozzles relative to fire and the distance between fire and the nearest set of jet fans. The last part consists of a few cases designed to verify the results obtained from the second part such that the model is producing reliable results. Each scenario is assigned a name for reference purpose.

3.10.1 Scenarios without Fire

In order to try to study the individual effect of fire, water mist system and tunnel ventilation system, test scenarios are run by isolating one of these components. Since preventing backlayering is the main focal of this project, the objective cannot be achieved without tunnel ventilation, therefore it is not useful to study scenarios in which tunnel ventilation is absent.

In Section 3.10.2, Test 17, 21 and 25 are already without water nozzles, therefore the effect of absence of water mist system can be studied via these cases. This section will then only describe the scenarios without fire.

In order to study how water droplets alone can affect the ventilation flow in tunnel, the cases in Table 4.5 are simulated without fire and the scenario names are listed in Table 3.4. The effect of drag reduction in FDS, as described in Section 3.2, is also studied by turning off the drag reduction model in FDS. It is hoped that these scenarios will show if the water droplets will slow the ventilation flow down due to drag.

Table 3.4: Scenarios with no fire

HGV Height (m)	Scenario Name according to Number of Water Nozzles			
	0	5	10	15
2.5	1	2	3	4
3.5	5	6	7	8
4.5	9	10	11	12

3.10.2 Main Scenarios

There is a set of base parameters used for comparison when varying other parameters, as listed in Table 3.5. When not mentioned for a scenario, the base parameters are assumed. For example, when only changing fire size, the height of HGV is 4.5 m, number of nozzles is 10 all located directly above HGV and the droplet median diameter is 200 μm etc. The adoption of these values is mostly explained in previous sections.

Table 3.5: Base simulation parameters

Parameter	Value
Design Fire Size	40 MW
HGV Height	4.5 m
Number of Water Mist Nozzles	10 (For spacing, refer to Fig. 3.9)
Water Mist Nozzle Locatoin	Above HGV
Water Droplet Median Diameter	200 μm
Distance between Nearest Set of Jet Fan to Fire Location	50 m

For design fire size, it varies from 20 to 60 MW, with 10 MW increment, as listed in Table 3.6.

Table 3.6: Design fire size scenarios

Design Fire Size (MW)	Scenario Name
20	13
30	14
50	15
60	16

Each combination of the height of vehicle on fire and number of water nozzles is tested to have a comprehensive understanding on how these two parameters interact with each other and affect backlayering, as listed in Table 4.5. The effect of vehicle height is studied to determine if the result is different among different vehicles, say between a passenger van and a heavy good vehicle. The arrangement of water nozzles is given in Fig. 3.9, for 5, 10 and 15 nozzles.

Table 3.7: HGV height and number of nozzles scenarios

HGV Height (m)	Scenario Name according to Number of Water Nozzles			
	0	5	10	15
2.5	17	18	19	20
3.5	21	22	23	24
4.5	25	26	27	28

Water mist nozzles are shifted to the upstream and downstream of HGV to determine how the location of where water droplets land will affect backlayering and the velocity, as listed in Table 3.8, as more water from upstream nozzles is likely to land near the fire

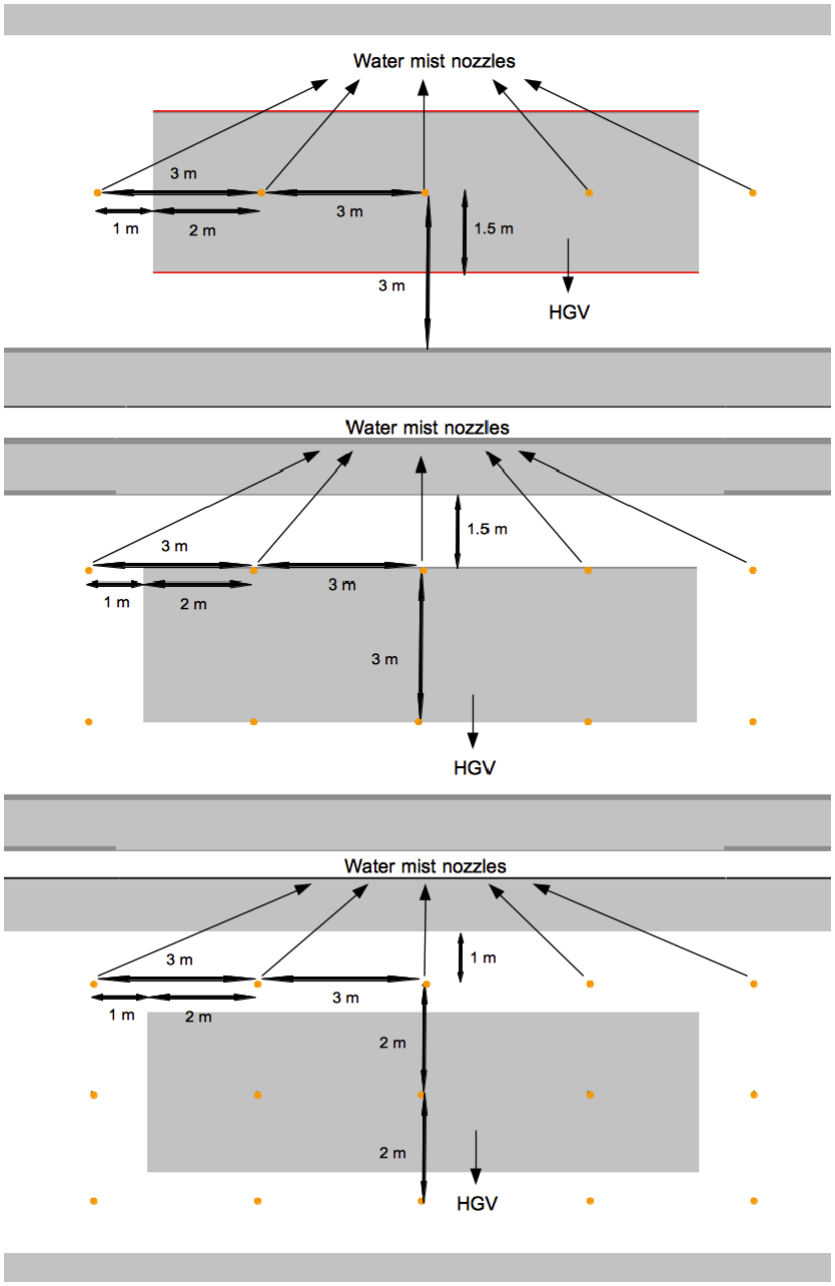

Figure 3.9: Plan view of nozzles above HGV, 5 nozzles (top), 10 nozzles (middle) and 15 nozzles (bottom)

seat under ventilation flow and water from downstream nozzles is not likely to land on the fire at all.

Table 3.8: Location of nozzles scenarios

Location	Scenario Name
10 m upstream of fire	29
10 m downstream of fire	30

The median diameter of water droplet is varied to 100 μm and 300 μm to test how gas cooling affects backlayering, as listed in Table 3.9.

Table 3.9: Water droplet size scenarios

Water Droplet Median Diameter (μm)	Scenario Name
100	31
300	32

3.10.3 Verification Tests

As explained in Section 3.5.3, the jet fans are activated one by one while allowing five minutes interval for the flow to stabilise. When backlayering stops occuring after a certain number of jet fans is activated, that number is deemed the minimum ventilation power required for that particular scenario. However in order to verify if the ventilation flow may slowly build up inertia force and hence dynamic pressure, resulting in incorrect results, and also if smoke will alter the flow pattern, the jet fans can be operated backwardly. In other words, in the verification scenarios, all jet fans are initially turned on and then turned off one by one at five minute interval. Once backlayering occurs after a certain number of jet fans is deactivated, that number plus one is the number of jet fans required to prevent backlayering. For example, if no backlayering occurs when six jet fans are on, and backlayering occurs when five jet fans are on, it can be deduced that six jet fans are required for that scenario. Only a few scenarios are chosen to be tested and the scenario names are listed in Table 3.10.

The second set of verification tests is grid sensitivity analysis which is performed in order to ensure the right grid resolution is used for the entire simulation. As a rule of thumb,

Table 3.10: Backwardly activated jet fans scenarios

Vehicle Height (m)	Number of Water Nozzles	Scenario Name
2.5	10	33
3.5	10	34
4.5	10	35
4.5	0	36

the simulation results will converge if the cell size is fine enough as most of the large eddies will be resolved in the simulation. One scenario is tested with coarser cells and one with finer cells, with the base scenario described in Table 3.5 and the cell sizes are described in Table 3.11.

Table 3.11: Grid resolution sensitivity analysis scenarios

Area	Coarse Scenario	Original Scenario	Fine Scenario
Fire and Nozzle Area	50 cm	25 cm	25 cm
Jet Fan Area	100 cm	50 cm	25 cm
Buffer Area	100 cm	50 cm	50 cm
Other Areas	100 cm	100 cm	100 cm

4 Results and Discussion

This section is structured according to the different types of scenarios, as stated in Section 3.10 and discussions are done within the respective sections. A conclusion is then presented at the end of the section to bring everything to a bigger picture to summarise the results.

4.1 Scenarios without Fire

The first set of results discussed here is the scenarios without fire, and the scenario descriptions were previously listed in Table 3.4. Only the velocity profile over height is analysed here as there is no smoke produced and therefore no backlayering. As mentioned in Section 3.9, the velocities were measured at 10 m upstream of the vehicle location over the entire tunnel cross section evenly, after the steady flow has been established. The objective here is to determine the impact of non-evaporating water to the ventilation flow.

As the difference in velocity when activating more nozzles was too small to be shown in a graph, the values of scenarios with no nozzle and percentage difference compared to the scenario without water is listed in Table 4.1, 4.2, and 4.3 for vehicle height of 2.5 m, 3.5 m and 4.5 m respectively.

Table 4.1: Velocity over tunnel height and percentage difference compared to scenario with no nozzle, for vehicle height of 2.5 m

Height in Tunnel (m)	0 Nozzle Velocity (m/s)	5 Nozzles % Difference	10 Nozzles % Difference	15 Nozzles % Difference
5	8.891	0.64	0.19	0.31
4	6.752	0.32	0.27	0.19
3	3.003	-2.62	-1.192	-2.73
2	1.016	4.72	-6.93	-7.06
1	0.453	3.47	3.14	-16.5

The result of vehicle height of 2.5 m is firstly analysed. As shown in Table 4.1, for the 5 nozzles scenario (Test 2), almost every velocities across the height have increased. This

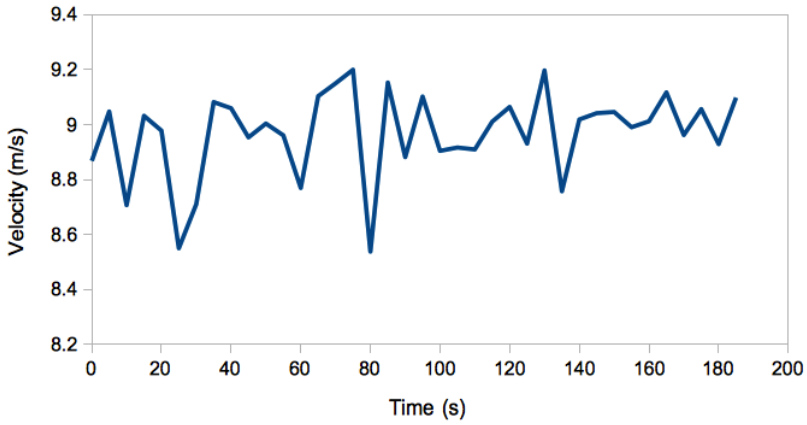

Figure 4.1: Fluctuation of velocity measurement over time for Test 2 at the height of 5 m

result is not expected, as the volatile particles are expected to have throttling effect on the flow and cause the flow velocities to drop. It can be explained that the momentum of particles is higher than the flow and instead of slowing the flow down, the momentum of particles is transferred to the flow and the flow is accelerated as a result. However it is also possible that the results were merely due to the fluctuating nature of turbulence model, as the percentage differences are all lesser than 7 %. The fluctuation of velocity measurement can be illustrated in Fig. 4.1, which shows the velocity at 5 m tall for Test 2 after backlayering was prevented and steady flow was established. The degree of fluctuation differed for every scenario.

The 10 nozzles scenario (Test 3) shows decrease in velocity for all heights compared to Test 2 and the velocities at 2 m and 3 m high are even lower than the ones in Test 1. For the 15 nozzles scenario (Test 4), the velocities at all height further decrease and velocities at 1 m, 2 m and 3 m high are all lower than Test 1.

The difference among Test 2, 3 and 4 is not only the amount of water injected into the tunnel, but also the density of water spray across the cross section, as each test has 1, 2 and 3 rows of water nozzles respectively. The decrease in velocities in Test 3 and 4 can be due to two reasons. Firstly, the collision among water droplets was larger when the spray was too close to each other and resulted in lower overall momentum, causing momentum transfer to happen from fluid to particles and slowing the fluid down. Sec-

ondly, the water volume for Test 3 and 4 was higher and therefore induced more drag to the flow and slowed the flow down. Currently it cannot be determined which of the above was the main cause that slowed the flow down because individual particle velocity cannot be measured in FDS and therefore the total momentum of the particles cannot be determined. Further experiments should be conducted to see how the density of water spray and their interaction affects the ventilation flow.

Table 4.2: Velocity over tunnel height and percentage difference compared to scenario with no nozzle, for vehicle height of 3.5 m

Height in Tunnel (m)	0 Nozzle Velocity (m/s)	5 Nozzles % Difference	10 Nozzles % Difference	15 Nozzles % Difference
5	8.835	0.07	0.59	0.20
4	6.705	0.51	-0.53	-0.311
3	2.970	2.64	-2.54	-2.97
2	0.900	0.56	1.24	0.23
1	0.296	12.7	4.42	-9.95

Table 4.3: Velocity over tunnel height and percentage difference compared to scenario with no nozzle, for vehicle height of 4.5 m

Height in Tunnel (m)	0 Nozzle Velocity (m/s)	5 Nozzles % Difference	10 Nozzles % Difference	15 Nozzles % Difference
5	8.731	-0.30	-0.27	-0.52
4	6.611	-0.25	-1.14	-0.52
3	2.874	-2.66	4.21	-2.61
2	0.734	-2.89	-7.08	3.06
1	-0.080	3.34	38.76	-0.72

For the result of vehicle height of 3.5 m, as shown in Table 4.2, for the 5 nozzles scenario (Test 6), there was a big increase in velocity of 12.7 % at 1 m, and then the velocity at the same height decreased to 4.42 % for 10 nozzles scenarios (Test 7) and -9.95 % for 15 nozzles (Test 8). The pattern was similar to the cases with vehicle height of 2.5 m, as the velocity at 1 m, 3m and 4 m was at the highest value when 5 nozzles were activated and slowly decreased with more number of nozzles activated and had lower velocities than the scenario without nozzle. The same set of explanations given for the 2.5 m vehicle are all applicable for the 3.5 m vehicle.

Finally for the result of vehicle height of 4.5 m, other than the big increase in velocity at height 1 m for 10 nozzles (Test 11) because the magnitude of those values was rather

small, there was a slight drop in velocity for most of the heights in all three cases. The overall pattern of change in velocity was quite different from other two tests as most velocity measurements were lower than without nozzle (Test 9), and was possibly due to water curtain effect. However increasing number of water nozzles did not result in even lower velocity. Comparison of velocity for tests with different vehicle heights and same number of nozzles is shown in Fig. 4.2. For all four comparisons, the velocities across the entire tunnel height were slightly lower when taller vehicle was used.

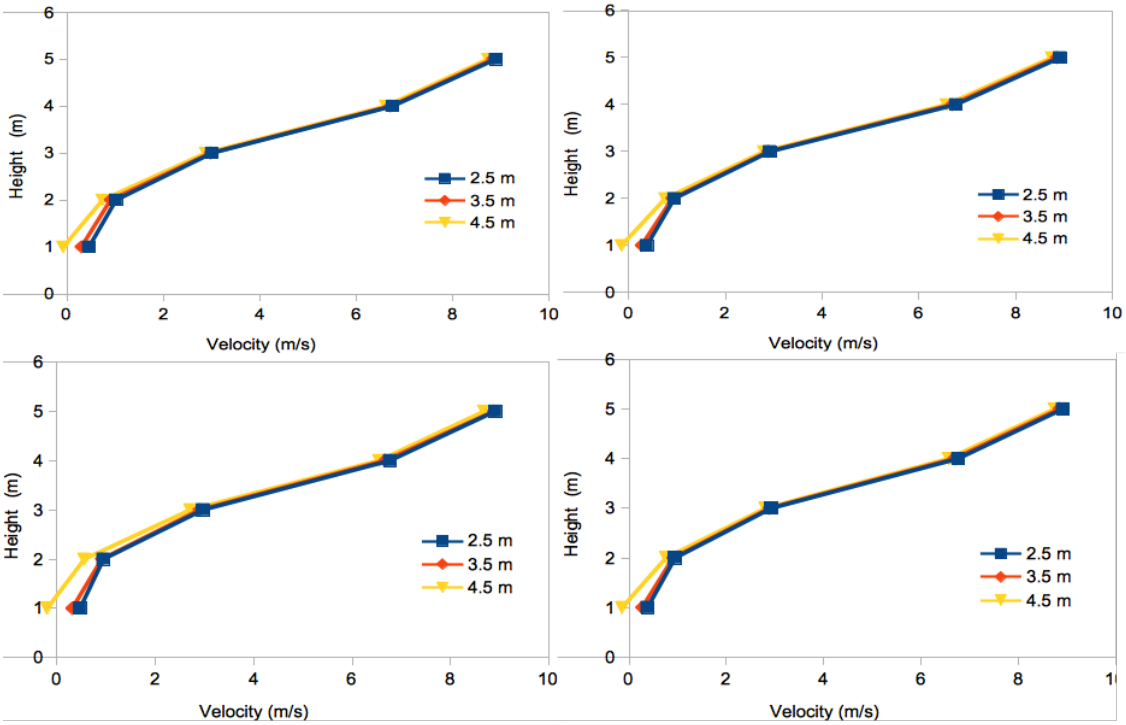

Figure 4.2: Longitudinal velocity across tunnel height for three different vehicle height under the influence of: Top Left: 0 nozzle; Top Right: 5 nozzles; Bottom Left: 10 nozzles and Bottom Right: 15 nozzles

FDS Particle files are plotted to visually determine how water droplets spread under ventilation, as shown in Fig. 4.3. As shown, there was a large gap between the top of the 2.5 m tall vehicle, a smaller gap for the 3.5 m vehicle and almost no gap for the 4.5 m vehicle. Also, the density of water droplets for the 4.5 m vehicle was also thicker. From this it can be therefore deduced that in order for water curtain effect to take place, the water spray has to be sufficiently dense.

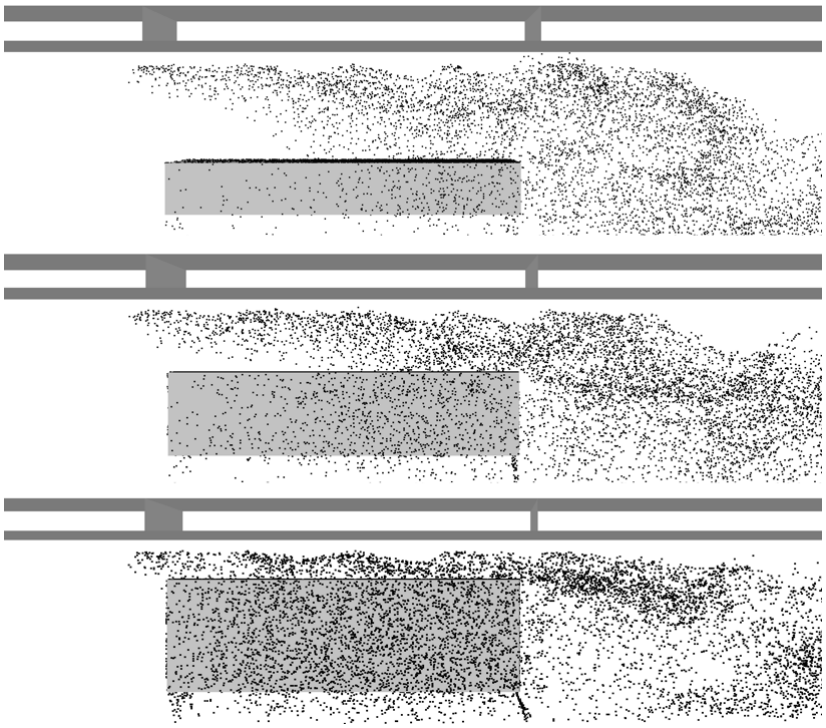

Figure 4.3: FDS Particle files showing water droplets in tunnel for three different vehicle heights: top: 2.5 m tall vehicle (Test 2); mid: 3.5 m tall vehicle (Test 6); bottom: 4.5 m tall vehicle (Test 10)

All in all, for this part, the water introduced to the tunnel seemed to slightly slow down the ventilation flow of the 4.5 m tall vehicle and it was most likely due to water curtain effect as there was almost no gap between the water droplets and the vehicle. For vehicle height of 2.5 m and 3.5 m, the results seemed random for 5 and 10 nozzles scenario and velocities at low level decreased for 15 nozzles scenario.

4.1.1 Scenarios without Drag Reduction Model

In order to examine the drag reduction model FDS uses to account for the aerodynamic interactions among particles when the separation distance is very small, as explained in Section 3.2, extra scenarios were simulated for all three vehicle heights with 15 nozzles by turning off the drag reduction model. The resultant flow is expected to have lower velocity than the previous scenarios as the flow experiences more drag from the particles. The results of these extra scenarios are listed in Table 4.4.

Table 4.4: Comparison of velocity over tunnel height for scenarios with drag reduction model turned on and off, for three vehicle heights

Height in Tunnel (m)	With Drag Reduction Model Velocity (m/s)	Without Drag Reduction Model % Difference
2.5 m tall vehicle		
5	8.918	3.25
4	6.765	-0.63
3	2.921	-0.2
2	0.945	-0.79
1	0.378	-0.27
3.5 m tall vehicle		
5	8.870	-0.08
4	6.703	-0.71
3	2.900	4.01
2	0.915	-8.90
1	0.282	-17.13
4.5 m tall vehicle		
5	8.760	-0.61
4	6.633	-0.29
3	2.856	4.70
2	0.750	-11.22
1	-0.084	37.14

The results shown in Table 4.4 showed that for most heights measured, the velocities without drag reduction model decreased, with a wide range of percentage difference. The high percentage difference measured at 1 m for 4.5 m vehicle was likely due to the small magnitude of the value. The results matched with the expectation that turning FDS drag reduction model off slowed the flow down as there was more drag when the flow passed by the dense particle array. However, based on the results above, the drag reduction did not cause significant difference to the flow velocity. It is noted that the drag reduction model FDS adopted was deemed to underestimate the reduction by Prahl et al. [50], however it was impossible to make comparison due to the lack of experiment result and FDS does not offer other options of drag reduction model.

The overall result of this section suggested that throttling effect due to only water mist system is not significant as the percentage differences between with and without nozzles were not huge. Additionally, turning on nozzles did not always result in lower flow velocity, in some cases turning on nozzles sped up the flow instead. There are a few ways

to explain the results. Firstly, it is possible that the amount of water introduced to the model was simply too little to affect the flow and the measurements were merely fluctuations in values. Secondly, instead of momentum transferring from flow to particles, the momentum of the droplets might be so high that it was transferred to the flow and thus accelerating the flow.

Another possibility is that FDS is not capable of simulating ventilation flow past a water curtain accurately, as the water droplets are lumped into larger Lagrangian particles for calculation and as a result not acting like a screen across the tunnel, as explained in Section 3.2. The other finding from the simulations was that the change in flow velocity depended largely on the vehicle height, as all three tested vehicles produced very different simulation results. Minor water curtain effect was observed in the 4.5 m tall vehicle case as velocities at most height decreased when added water mist nozzles into the simulations.

Ultimately the level of confidence that FDS correctly simulated the water curtain effect is not high, as there is lack of experimental result to make comparison with and it was uncertain that the simulation result was physically correct due to the lack of obvious pattern. In future, more experiments shall be carried out to study the flow passing dense water mist spray and to study the drag reduction effect. However note that these scenarios were tested without fire and the effect of additional water vapour evaporated due to hot smoke is unclear. It is practically impossible to isolate the influence of evaporated water vapour mass alone as it is always coupled with gas cooling effect on fire and smoke layer.

4.2 Scenarios with Varying Vehicle Height and Number of Water Nozzles

The result of this section is presented in a matrix form since every combination of the variables (vehicle height and number of water nozzles) are tested, as shown in Table 4.5.

Table 4.5: Number of jet fans required for different vehicle height and number of water nozzles

Vehicle Height (m)	Number of Water Nozzles			
	0	5	10	15
2.5	4	4	4	3
3.5	4	4	4	4
4.5	6	6	5	4

For a 2.5 m tall vehicle, the number of jet fans required to prevent backlayering reduced from 4 to 3 when 15 nozzles were used. Similarly, for a 4.5 m tall vehicle, number of jet fans required reduced from 6 to 5 when using 10 nozzles and to 4 when using 15 nozzles. The reduction was most likely due to the more gas cooling effect on smoke layer when more nozzles were deployed, as shown in Fig. 4.4 and 4.5, as the gas temperature was lower when more nozzles were deployed.

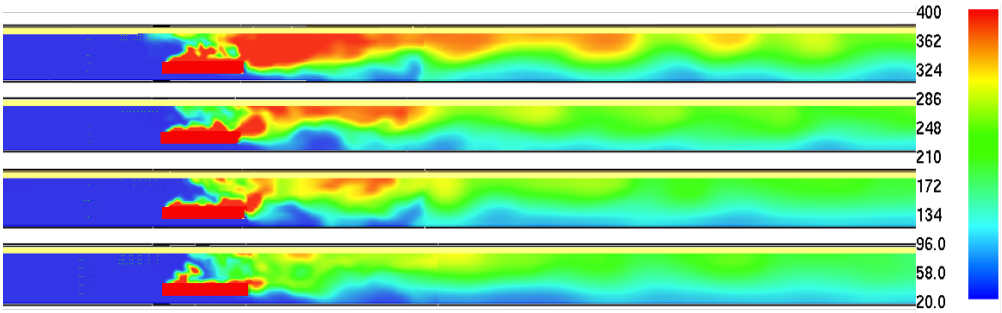

Figure 4.4: Temperature slice file on the scale of 20°C to 400°C of a 2.5 m tall vehicle, in the order of 0 nozzle, 5 nozzles, 10 nozzles and 15 nozzles

It was unclear why, for the 3.5 m vehicle, the number of jet fans required did not reduce with the increase of water nozzles.

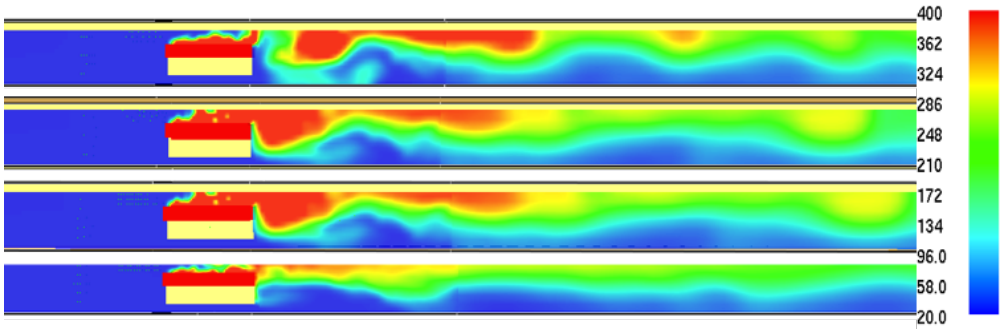

Figure 4.5: Temperature slice file on the scale of 20°C to 400°C of a 4.5 m tall vehicle, in the order of 0 nozzle, 5 nozzles, 10 nozzles and 15 nozzles

The velocity profile over height when backlayering was prevented is shown in Fig. 4.6 for all three vehicle heights. For the 2.5 m tall vehicle, there was a significant increase in velocity at high level (4 m and 5 m), and decrease at low level (1 m and 2 m) when 10 and 15 nozzles were used. These flow patterns were quite similar to the tests without fire, as explained in Section 4.1. The further decrease in velocity when 15 nozzles were used compared to the 10 nozzles case was likely due to the lesser number of jet fans required to prevent backlayering (3 instead of 4).

For the 3.5 m tall vehicle the flow pattern was entirely different from the 2.5 m one, as the velocities were almost straight lines ranging from 2.5 to 3.1 m/s, with the highest velocity at middle level. The differences between tests were very small as the number of jet fans required was the same for all tests.

Similar to the 3.5 m tall vehicle tests, the velocity profile for the 4.5 m tall vehicle was rather flat, with a slight increase in negative gradient, with the largest difference in absolute value not more than 30% for any tests. However due to the decrease of required jet fans with increasing number of nozzles, the velocity also decreased accordingly at every height. This agreed with the conclusion of a study by Wu and Hsu [35] that higher water flow density leads to lower critical velocity. Although water flow density does not change in this study, increasing number of nozzles is effectively causing higher water flow rate, which is the same effect as increasing water flow density. Besides that, the additional

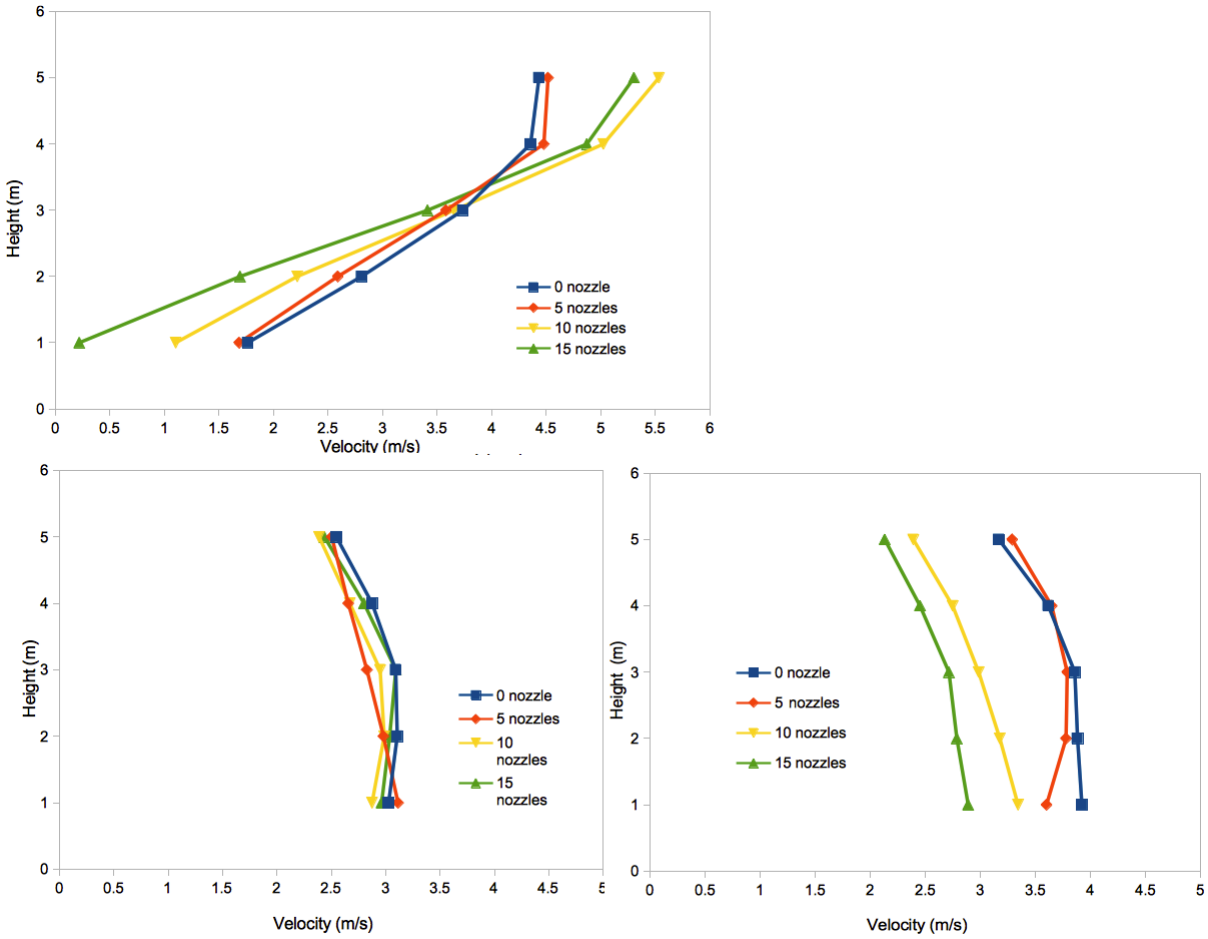

Figure 4.6: Longitudinal velocity across tunnel height for three different vehicle height under influence of different number of nozzles. Top: 2.5 m tall vehicle; bottom left: 3.5 m tall vehicle; bottom right: 4.5 m tall vehicle

water vapour mass in the smoke layer and water curtain effect seemed to have little to no effect on the result as there was no case in which more jet fans was required than the test without any nozzle.

On the other hand, as shown in Table 4.5, by raising the height of the vehicle, the number of jet fan required to prevent backlayering also increased, regardless of how many water nozzles were used. For instance, when five nozzles were used, it requires 4 fans for a 3.5 m tall vehicle and 5 fans for a 4.5 m tall vehicle. It can be due to the larger backlayering length that the taller vehicles caused.

Although in Eq. 8 the only factors affecting the backlayering length are the heat release

rate, longitudinal ventilation velocity and tunnel height, for calculating dimensionless quantities, the equation is only valid when there is no obstruction in the tunnel and does not address the effect of the height of fire. However it is very likely that when the base of fire is heightened, the further the ceiling jet and flame extension will spread, just like the flame extension is larger in a compartment fire when the distance between base of fire and ceiling is shorter [53].

In order to determine how the vehicle height will affect the backlayering length in FDS, additional tests were conducted using no water nozzle and only two jet fans for each vehicle height. Two jet fans were used because it will not prevent backlayering for all three heights and using the same number of jet fans will make a fair comparison across different tests. The FDS SMOKE3D files of the tests are shown in Fig. 4.7.

The result showed that the backlayering length increased a lot when taller vehicles were used. The slice files of longitudinal velocity, as shown in Fig. 4.8, also showed that the taller vehicles edin higher longitudinal velocity of smoke. Note that the scale in the figure is from -6 to 0 m/s, therefore areas with positive velocity were in red. It can then be explained that the more backlayering was, the more resistance hot smoke created to impede the ventilation flow and therefore more jet fans were required to prevent backlayering.

If Eq. 8 is modified with the tunnel height replaced by the height between the ceiling of tunnel to base of fire, the backlayering length l^* then relates to the height H with this relationship: $l^* \propto ln(\sqrt{H})$ when $Q^* > 0.15$, which is clearly wrong as proven above. This shows that the height of the fire surface has to be taken into account explicitly when calculating backlayering length and new equations shall be formulated similar to the equations used in enclosure fire dynamics in the future.

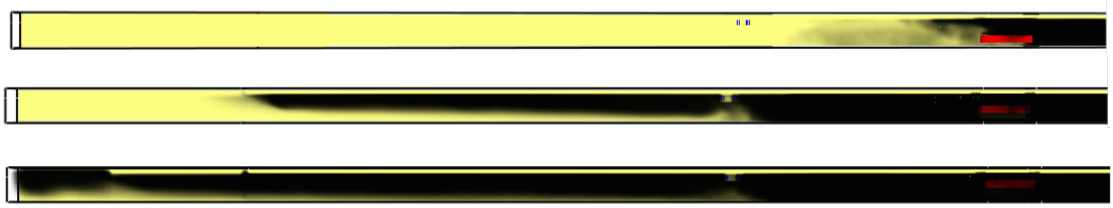

Figure 4.7: Comparison of FDS SMOKE3D files when simulating 2 jet fans for different vehicles. Top: 2.5 m tall vehicle; mid: 3.5 m tall vehicle; bottom: 4.5 m tall vehicle

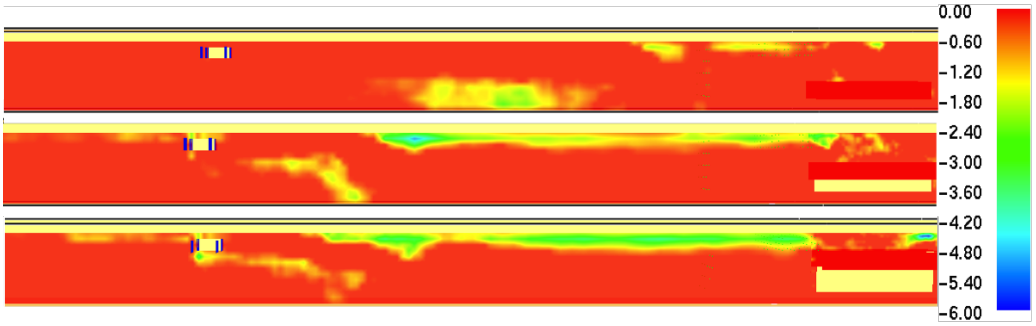

Figure 4.8: Comparison of slice files of longitudinal velocity on the scale of -6 to 0 m/s when simulating 2 jet fans for different vehicles. Top: 2.5 m tall vehicle; Mid: 3.5 m tall vehicle; Bottom: 4.5 m tall vehicle

The result in Figure 4.8 can also be used to explain the difference in gradient of velocity over height for different vehicle heights, as shown in Fig. 4.6, as the velocities were at the highest at high level and at the lowest at low level for 2.5 m tall vehicle, and exact opposite outcome for 3.5 m and 4.5 m tall vehicle. With lesser backlayering, the result for 2.5 m vehicle was similar to the one without fire, as the hot smoke had little influence on the ventilation. For 3.5 m vehicle, the cold jet fans flow bent downwards to lower pressure zone when obstructed by high velocity smoke and causing the velocity at the low level to increase. Even after backlayering was prevented, the ventilation flow still bent down near the fire. It was unsure why the high velocity jet fan flow did not revert to the original path after all the smoke was pushed back. An example slice file of longitudinal velocity over time, as Fig. 4.9, showed the change in ventilation flow direction. The flow pattern for the 4.5 m vehicle was similar to the 3.5 m one, except with larger deflection on the jet fan flow.

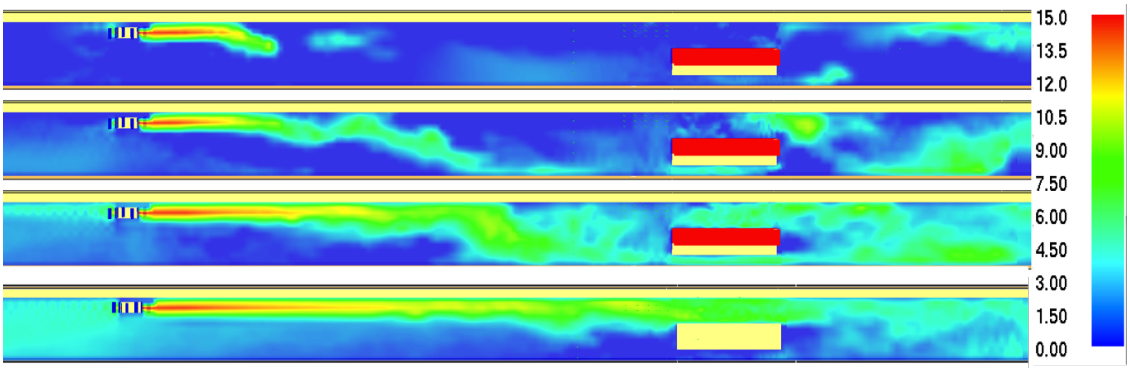

Figure 4.9: Comparison of slice files of longitudinal velocity for 3.5 m vehicle at different times when there is fire and steady state without fire. In order: before jet fan flow interacts with smoke; after jet fan flow interacts with smoke, before backlayering is prevented; after backlayering is prevented and when there is no fire.

4.3 Scenarios with Varying Nozzles Location

The number of jet fans required to prevent backlayering for different nozzle locations and vehicle heights is summarised in Table 4.6.

Table 4.6: Number of jet fans required for different nozzle locations and vehicle height

Nozzle Location	Number of Jet Fan Required
Upstream of Fire	6
Directly above Fire	5
Downstream of Fire	4

The number of jet fan required Injecting water upstream was expected to have more water landing on the fuel surface under longitudinal ventilation at the cost of creating turbulence, slowing the flow down and less gas cooling since lesser water droplets will fall in the smoke layer. Since this simulation has a fixed heat release rate for every scenario, the effect of more water landing on the fuel surface for fuel cooling was not simulated, and only the effect of extra turbulence and gas cooling can be determined. However as water mist system was tested here, in reality most fine droplets are not expected to land on the fuel surface due to lower terminal velocity and most droplets will evaporate very quickly. Therefore it is reasonable to only look at the latter two effects. Also the effect of water mist system blocking the smoke is not expected because of the presence of longitudinal ventilation, according to Sun et al. [31]

The turbulence created by the water mist injected upstream can be seen in Fig. 4.10, which is the comparison of FDS SMOKE3D files between placing the water nozzles directly above the fire and upstream. Smoke stratification was lost when water droplets were injected at the upstream of fire, as the water droplets flushed the smoke down and also as the temperature stratification was less significant after the smoke was cooled down, as discussed in Section 2.1.

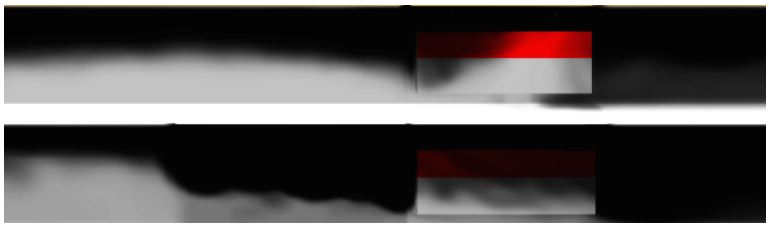

Figure 4.10: Comparison of FDS SMOKE3D file when placing water nozzles at different locations. Top: Directly above fire; bottom: 10 m Upstream of fire

The amount of water evaporated, as shown in Table 4.7, showed the big difference when placing nozzles at different location. It cannot be determined if the effect of turbulence created or less gas cooling was the main reason of causing more jet fans needed at upstream since both effects happened at the same time and cannot be decoupled.

Table 4.7: Amount of water evaporated when injected from different locations

Nozzle Location	Mass of Evaporated Water (kg)
Upstream of Fire	8.23
Directly above Fire	21.79
Downstream of Fire	35.10

When placing the nozzles at downstream, it required one less jet fan to prevent backlayering. This result coincided with the result in Table 4.5, as 1 less jet fan was required when using 15 nozzles compared to 10 nozzles. This was expected as more water droplets landed in the smoke layer under the influence of tunnel ventilation when the nozzles are placed at downstream and result in more gas cooling, as seen in Table 4.7. Also there was lesser turbulence created around the fire location when the nozzles were placed at the downstream.

The results in this section showed that the recommendation in *Engineering Guidance for Water Based Fire Fighting Systems for the Protection of Tunnels and Subsurface Facilities* [4] that the water nozzles should be activated both at the upstream and downstream of fire is not applicable to water mist system. However the same conclusion cannot be made for water deluge system since fuel cooling will be an important and non-negligible cooling mechanism and it was not simulated in this project.

4.4 Scenarios with Varying Design Fire Size

The number of jet fans required in order to prevent backlayering for different design fire size is summarised in Fig. 4.11.

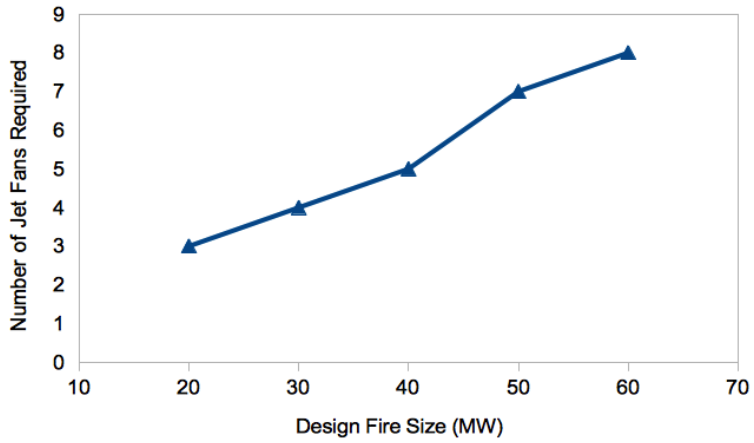

Figure 4.11: Number of jet fans required for different design fire size

As seen from the result, the number of jet fan required almost linearly increased with increasing fire size. This was the same as the conclusion of the study by Vaitkevicius et al. [23], which is a similar study to this project except that there was no presence of water mist system in their study. The mass of water evaporated from nozzles was also very similar for all three cases, which was sensible because the water flow rate was identical for all three cases, and air temperature directly above the fire was very high for all three fire size and would evaporate the water droplets very quickly. This result also showed that adding water mist to fire did not suppress fire throttling effect which is more significant at larger fire size as more heat and volatile particles are added to the

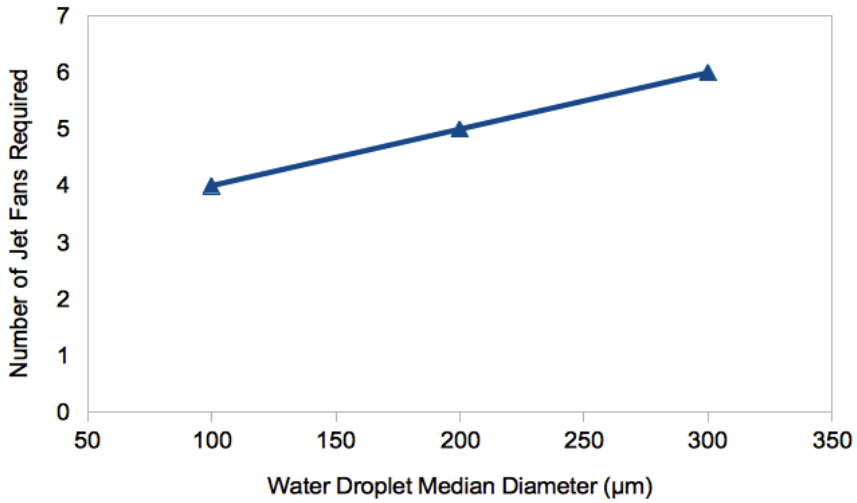

Figure 4.12: Number of jet fans required for different water droplet size

tunnel.

According to the equations proposed by Oka and Atkinson [9], and Wu and Bakar [10], as discussed in Section 2.3.3, the critical velocity is constant beyond certain fire size. For the tunnel of this simulation the corresponding fire size is 11.9 MW and 19.8 MW for both theories using Eq. 2 and 3. The result from this section was clearly incompatible with these theories as the number of jet fans required to prevent backlayering kept increasing beyond the theoretical fire size, which means the theory of super critical velocity is not feasible when designing real longitudinal ventilation system as the theory does not take the fire throttling effect on ventilation system into account.

4.5 Scenarios with Varying Water Droplet Size

Three different water droplet median diameters, 100, 200 and 300 μm were tested using the base set of parameter, and the result is shown in Fig. 4.12.

Figure 4.13 shows the amount of water vapour evaporated from nozzles and Fig. 4.14 shows the longitudinal velocity distribution over height for different diameters.

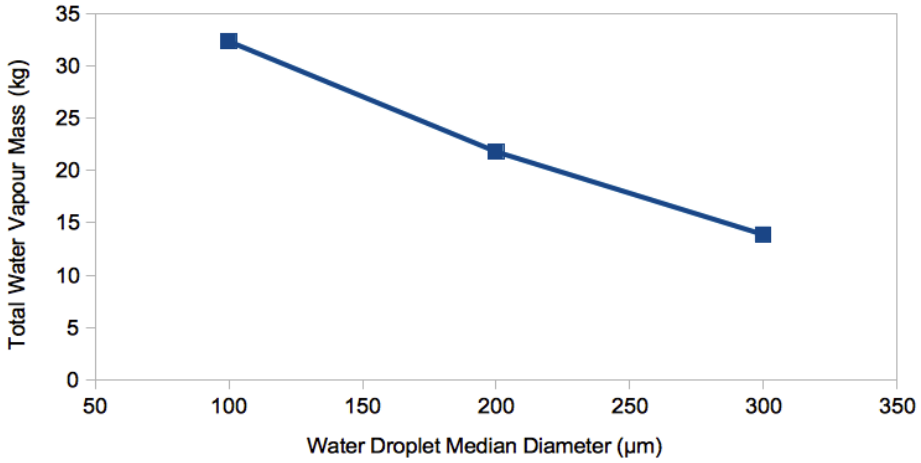

Figure 4.13: Water vapour mass without backlayering for different water droplet size

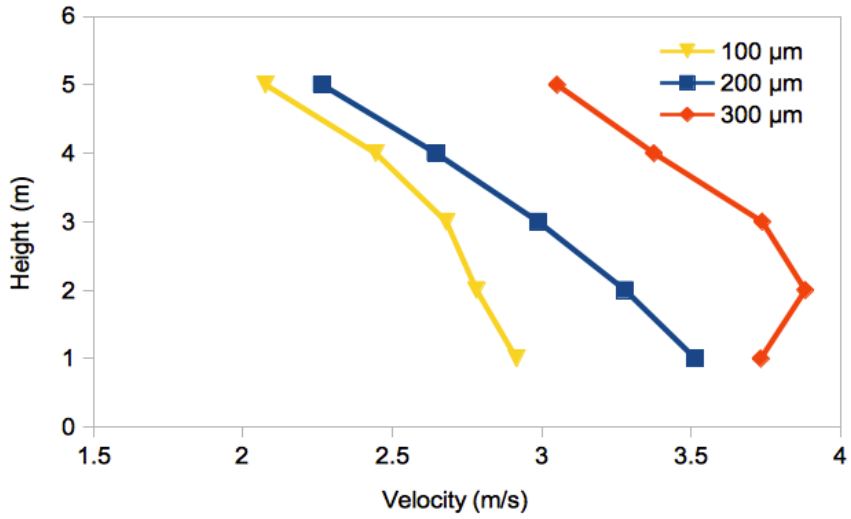

Figure 4.14: Longitudinal velocity distribution over height without backlayering for different water droplet size

As shown in Fig. 4.13, the smaller the diameter of water droplet was, the more water vapour evaporated. Even though the total mass of water injected by nozzles only depends on the K-factor and operating pressure, both not varied in these scenarios, with smaller droplets there was more water vapour created. This was due to the ability of smaller droplets to absorb more heat as its surface to volume ratio is significantly higher than larger droplets'. The difference in the ratio between two droplet sizes is equal to R_2/R_1, therefore a 100 μm droplet has twice as high surface to volume ratio as a 200 μm droplet. However the ratio of water vapour mass between 100 μm and 200 μm from the simulation result was only 1.48 and ratio between 100 μm and 300 μm was only 2.32, suggesting that an extra correlation factor is required to formulate the relationship between water droplet size and how much water evaporates in smoke. Further discussion is out of the scope of this project.

The decrease in longitudinal velocity when using smaller droplets, as shown in Fig. 4.14, agreed with the finding of Wu and Hsu's study [35] that the critical velocity decreases with the droplet size. Despite that their simulation was done using a velocity boundary vent at the tunnel portal, it is safe to say that the decreasing pattern on both studies was caused by the decrease in water droplet size. Although their study used droplet size of the range from 800 to 1200 μm, the result here further extended the range of their conclusion.

The gas cooling effect can be also demonstrated via temperature slice files across the longitudinal direction of the tunnel, in Fig. 4.15. The slice files show that the gas temperature when using 100 μm was the lowest compared to the other two, as the area in red did not extend as far out as the other two cases. This shows that with smaller water droplet, gas cooling was more effective.

As lesser jet fans were required to prevent backlayering when smaller droplets were used, it can be concluded that the gas cooling effect dominated over the potential throttling

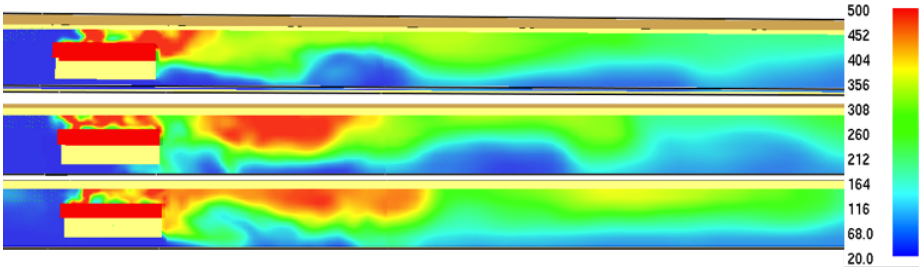

Figure 4.15: Temperature slice file on the scale of 20°C to 500°C across the longitudinal direction. Top: 100 μm; Mid: 200 μm; Bottom: 300 μm

Table 4.8: Comparison of number of jet fans required for backwards activation tests and the corresponding original tests

Test Name	Original Test	Verification Test
33	4	4
34	4	4
35	5	5
36	6	6

effect caused by extra water vapour mass and it therefore required lesser jet fans to prevent backlayering when smaller droplets were used.

4.6 Verification Tests

4.6.1 Backwards Activation

The number of jet fans required by Test 33-36 compared to their original scenarios is all summarised in Table 4.8. As seen, it required the same number of jet fans to prevent backlayering regardless of the jet fan activation sequence.

The comparisons of velocity profile over height is shown in Fig. 4.16. The velocity profile looked similar for all the scenarios, given that the velocity measurement in FDS fluctuated a lot over time, it is reasonable to conclude that the flow pattern was not affected by the activation sequence.

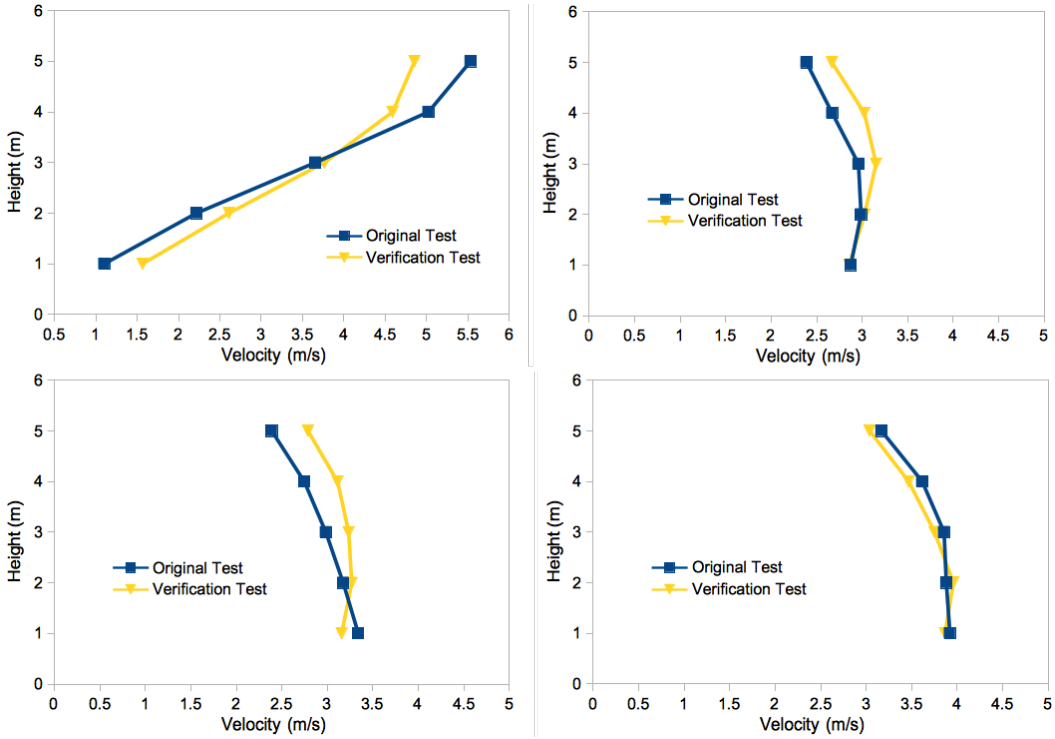

Figure 4.16: Comparisons of velocity profile over height between original and verification test for various scenarios. Top left: 2.5 m vehicle with 10 nozzles; top right: 3.5 m vehicle with 10 nozzles; bottom left: 4.5 m vehicle with 10 nozzles and bottom right: 4.5 m vehicle with no nozzle

4.6.2 Grid Resolution Sensitivity Analysis

The number of jet fans required for the coarse, original and fine mesh tests is summarised in Table 4.9 and the velocity profile over height is plotted in Fig. 4.17. The percentage discrepancy of the velocity between the original and fine mesh is calculated in Table 4.10.

Table 4.9: Comparison of number of jet fans required for grid sensitivity analysis tests

Test	Number of Jet Fan Required
Coarse	3
Original	5
Fine	5

As seen, the result from the coarse test was very different from the original and fine test, proving that meshes coarser than the original ones should not be used. Comparing the results of original and fine test, it can be concluded that the two sets of results were

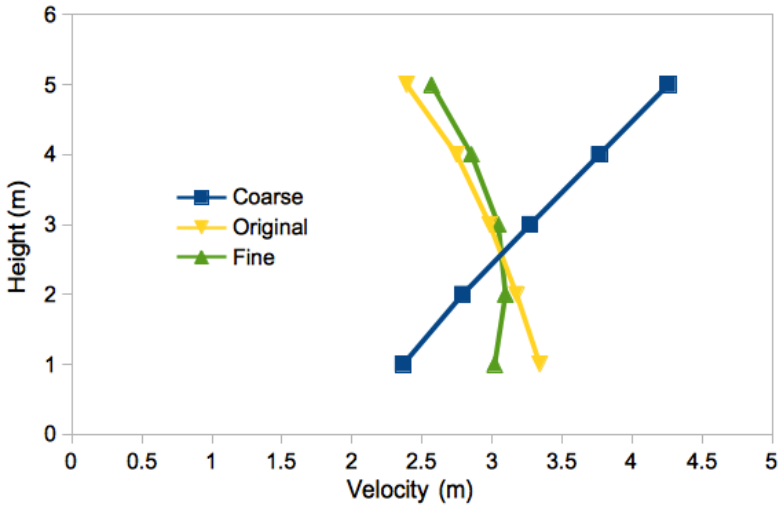

Figure 4.17: Velocity profile over height for scenarios with different meshes

Table 4.10: Percentage discrepancy of velocity over height between the original and fine test

Height (m)	Velocity in Fine Test (m/s)	Percentage Discrepancy with Original Test (%)
5	3.02	10.66
4	3.10	2.56
3	3.04	-2.00
2	2.85	-3.70
1	2.57	-6.96

almost converging and the original meshes were fine enough for the simulation. Also, the fine test took triple the time of the original test.

The results from these two verification tests provided a high level of confidence in the overall methodologies and results in this project. However, in order to validate the results of this project, it is recommended that small and large scale experiments are to be done. Small scale experiments are particularly useful as there are many variables involved and large scale experiments will take huge amount of resource to complete.

5 Conclusions and Further Research

The main purpose of this project is to serve as a general practical guide for engineers when designing the tunnel life safety system and strategy. Fire Dynamics Simulator (FDS) Version 6.5.3 simulations have been carried out to investigate the interactions among tunnel longitudinal ventilation system, water mist system and fire, with the objective of preventing smoke backlayering. A heavy good vehicle (HGV) has been used as the fire source and placed close to the jet fans, as it is deemed to be the worst case scenario.

A few general conclusions have been deduced from this project:

- In the absence of fire, the effect of introducing water mist droplets in the middle of tunnel, acting as a water curtain, was uncertain. This was due to the lack of obvious patterns from the simulation results, the lack of experimental results to compare with and the lack of confidence that FDS is capable of simulating drag induced by fine water droplets correctly.
- Taller vehicles required more jet fans to prevent backlayering, thus in a tunnel, vehicles such as trucks and HGV possess the biggest challenge when designing longitudinal ventilation system. This was largely due to the larger backlayering length that taller vehicles on fire caused.
- The velocity profile over height changed completely when the height of the vehicle was varied.
- Number of jet fans required reduced with the increase of water mist nozzles, regardless of vehicle height, due to greater gas cooling effect.
- Placing the water mist nozzles at the upstream of fire resulted in more jet fans required, due to the extra turbulence created when water droplets penetrated the smoke layer and lesser gas cooling effect as lesser water droplets landed in the smoke layer. On the opposite, placing the nozzles at the downstream resulted in lesser jet fans required, for the same reasons. Therefore it is recommended to only

activate the water mist system at the downstream of fire when fire is detected if tunnel ventilation system is also activated simulanteously.

- Increasing the fire size resulted in more jet fans required, due to the fire throttling effect, even for fire sizes beyond the super critical region where critical velocity will remain constant regardless of fire size.
- Decreasing the water droplet size caused more gas cooling and therefore reducing the number of jet fans required.

There are a few limitations of the simulation in this project, therefore they have to be considered before applying the results into real life design:

- Due to the modelling of constant heat release rate, a few phenomena that were previously observed in experiments could not be accurately simulated, such as the flame suppression or extinguishment by water mist system, fire size enhancement in the presence of forced ventilation, etc.
- Water mist droplets are lumped into larger Lagrangian particles in FDS to save computational time. It is unsure if the drag force of flow passing fine water droplet array is accurately simulated in the software.
- The effect of using time-varying parameters, such as growing fire size, jet fans ramping up or zone activation of water nozzles were not studied in this project.
- The fire location was always near the jet fans in this project, it is unclear if the aforementioned conclusions still hold if the fire is located far away from the jet fans such that steady flow can be established before reaching the fire.

In the future, more researches should be conducted in the following directions:

- CFD simulation to further study the effects of other parameters such as spacing of nozzles, distance between fire location and jet fan and nozzles discharge direction. It is hoped that all the possible parameters can be placed together to form a complete picture.

- Experiments to validate the velocity measurement in FDS when flow passes through water mist spray.
- Small scale experiments to test if the conclusions made in this project are correct, especially the parts with varying vehicle height and nozzle location.
- Large scale experiments to validate the small scale experiments and formulate a few relationships currently not present to quantitatively describe the parameters related to tunnel fire dynamics, especially the factor of height of fire.
- Validation of FDS after the experiments above are done especially on the interaction between smoke and water mist droplets.

6 Acknowledgement

I have many people to thank in support of my thesis and IMFSE programme.

First of all, I would like to thank my thesis promoter, Dr Ricky Carvel for his endless professional advice and knowledge during these five months period. It is my priviledge to work with you to explore this interesting topic. I would also like to thank Mr Ben Ralph for his extraordinary knowledge in FDS and for providing me help whenever he could.

I would also like to thank Ms Ruth Wong for bringing me into Arup Singapore and supported my master's study. I look forward to continue my career under your supervision.

Last but not least, million thanks to my family and friends and I won't be who I am today without all of you.

7 References

[1] Haukur Ingason, Ying Zhen Li, and Anders Lnnermark. *Tunnel fire dynamics*. Springer, 2015.

[2] H Ingason and A Lönnermark. Heat release rates in tunnel fires: a summary. *Handbook of Tunnel Fire Safety*, (1994):309–328, 2012.

[3] *NFPA 502: standard for road tunnels, bridges, and other limited access highways*. NFPA, Quincy, MA, 2013.

[4] The Research Project UPTUN. Engineering Guidance for Water Based Fire Fighting Systems for the Protection of Tunnels and Subsurface Facilities. Technical Report August, The European Commission, 2007.

[5] Kevin Mcgrattan and Randall Mcdermott. Sixth Edition Fire Dynamics Simulator User's Guide. 2016.

[6] Richard Carvel and Guy Marlair. Chapter 1 A history of fire incidents in tunnels. In Alan Beard and Richard Carvel, editors, *Handbook of Tunnel Fire Safety*, chapter 1, pages 3–23. ICE Publishing, Edinburgh, 2nd editio edition, 2003.

[7] Beard Alan and Carvel Richard. A history of fire incidents in tunnels. In *Handbook of Tunnel Fire Safety*, pages 2–2. ICE Publishing, 2nd edition edition, 2012.

[8] CETU. Water mists in road tunnels: State of knowledge and provisional assessment elements regarding their use. (June), 2010.

[9] Graham T. Oka, Yasushi; Atkinson. Control of smoke flow in a tunnel. *Journal of Applied Fluid Mechanics*, 6(1):49–60, 2013.

[10] Y. Wu and M. Z.A. Bakar. Control of smoke flow in tunnel fires using longitudinal ventilation systems - a study of the critical velocity. *Fire Safety Journal*, 35(4):363–390, 2000.

[11] Ying Zhen Li, Bo Lei, and Haukur Ingason. Study of critical velocity and backlayering length in longitudinally ventilated tunnel fires. *Fire Safety Journal*, 45(6-8):361–370, 2010.

[12] S Jagger and G Grant. *Use of tunnel ventilation for fire safety.* 2012.

[13] Lee Chaiken 1979 Comb Sci Technol.pdf. *Combustion Science and Technology*, 20:59–72, 1979.

[14] F Colella, G Rein, and V Verda. Design of tunnel ventilations systems for fire emergencies using multiscale modelling. *Fourth International Symposium on Tunnel Safety and Security, Frankfurt am Main, Germany.*, 2010.

[15] Horst Starke. Fire Suppression in Road Tunnel Fires by a Water Mist System Results of the SOLIT Project. pages 311–321, 2010.

[16] Robert Hart. Numerical modelling of tunnel fires and water mist suppression. (December), 2010.

[17] Jeffrey S. Newman. Experimental evaluation of fire-induced stratification. *Combustion and Flame*, 57(1):33–39, 1984.

[18] Igor Maevski and Raymond C Klein. Impact of Tunnel Ventilation on Tunnel Fixed Fire Suppression System.

[19] G. T. Atkinson and Y. Wu. Smoke control in sloping tunnels. *Fire Safety Journal*, 27(4):335–341, 1996.

[20] Yee Ping Lee and Kuang Chung Tsai. Effect of vehicular blockage on critical ventilation velocity and tunnel fire behavior in longitudinally ventilated tunnels. *Fire Safety Journal*, 53:35–42, 2012.

[21] O. Vauquelin and D. Telle. Definition and experimental evaluation of the smoke "confinement velocity" in tunnel fires. *Fire Safety Journal*, 40(4):320–330, 2005.

[22] Francesco Colella, Guillermo Rein, Romano Borchiellini, and Jose L. Torero. *A Novel Multiscale Methodology for Simulating Tunnel Ventilation Flows During Fires*, volume 47. 2011.

[23] Arnas Vaitkevicius, Francesco Colella, and Ricky Carvel. Investigating the Throttling Effect in Tunnel Fires. *Fire Technology*, 52(5):1619–1628, 2016.

[24] R. O. Carvel, A. N. Beard, P. W. Jowitt, and D. D. Drysdale. Variation of heat release rate with forced longitudinal ventilation for vehicle fires in tunnels. *Fire Safety Journal*, 36(6):569–596, 2001.

[25] R O Carvel, A N Beard, and P W Jowitt. The effect of forced longitudinal ventilation on a HGV fire in a tunnel. *Proc. Int. Conf. on Tunnel Fires*, pages 191–200, 1999.

[26] Haukur Ingason and Ying Zhen Li. Model scale tunnel fire tests with longitudinal ventilation. *Fire Safety Journal*, 45(6-8):371–384, 2010.

[27] J. Qin and W. K. Chow. Bench-scale tests on PMMA fires with water mist. *Polymer Testing*, 24(1):39–63, 2005.

[28] Z. Jiang, W. K. Chow, J. Tang, and S. F. Li. Preliminary study on the suppression chemistry of water mists on poly(methyl methacrylate) flames. *Polymer Degradation and Stability*, 86(2):293–300, 2004.

[29] Zhen Wang. Optimization of Water Mist Droplet Size. 2015.

[30] Ir Victor Meeussen and Ir Tony Lemaire. The effect of a water mist system on large-scale tunnel fires. (August 2006):211–225, 2008.

[31] Jiayun Sun, Zheng Fang, Zhi Tang, Tarek Beji, and Bart Merci. Experimental study of the effectiveness of a water system in blocking fire-induced smoke and heat in reduced-scale tunnel tests. *Tunnelling and Underground Space Technology*, 56:34–44, 2016.

[32] Lvyi Chen, Wei Zhu, Xin Cai, Liwei Pan, and Guangxuan Liao. Experimental study of water mist fire suppression in tunnels under longitudinal ventilation. *Building and Environment*, 44(3):446–455, 2009.

[33] Peihong Zhang, Xing Tang, Xiangliang Tian, Chang Liu, and Maohua Zhong. Experimental study on the interaction between fire and water mist in long and narrow spaces. *Applied Thermal Engineering*, 94:706–714, 2016.

[34] G. Crosfield, R.; Cavallo, A.; Colella, F.; Carvel, R.; Torero, J.L.; Rein. Landing Distance of Droplets from Water Mist Suppression Systems in Tunnels with Longitudinal Ventilation. *Most*, 2009.

[35] Guan-yuan Wu and Shang-chin Hsu. The analysis of the effects of critical velocity in tunnel fires with water spray system.

[36] C. C. Hwang and J. C. Edwards. The critical ventilation velocity in tunnel fires - A computer simulation. *Fire Safety Journal*, 40(3):213–244, 2005.

[37] C. C. Hwang and J. D. Wargo. Experimental study of thermally generated reverse stratified layers in a fire tunnel. *Combustion and Flame*, 66(2):171–180, 1986.

[38] Esther Kim, John P. Woycheese, and Nicholas A. Dembsey. Fire dynamics simulator (version 4.0) simulation for tunnel fire scenarios with forced, transient, longitudinal ventilation flows. *Fire Technology*, 44(2):137–166, 2008.

[39] M Bilson, Andrew Purchase, and C Stacey. Deluge system operating effectiveness in road tunnels and impacts on operating policy. pages 167–174, 01 2008.

[40] Y Z Li and H Ingason. Numerical Simulation of Runehamar Tunnel Fire Tests. pages 203–210, 2012.

[41] Sung Chan Kim and Hong Sun Ryou. An experimental and numerical study on fire suppression using a water mist in an enclosure. *Building and Environment*, 38(11):1309–1316, 2003.

[42] Simo Hostikka and Kevin McGrattan. Numerical modeling of radiative heat transfer in water sprays. *Fire Safety Journal*, 41(1):76–86, 2006.

[43] Jason Floyd and Randall Mcdermott. Development and evaluation of two new droplet evaporation schemes for fi re dynamics simulations. *Fire Safety Journal*, 91(February):643–652, 2017.

[44] Peter Sturm, Michael Beyer, and Mehdi Rafiei. On the problem of ventilation control in case of a tunnel fire event. *Case Studies in Fire Safety*, 7:36–43, 2017.

[45] A. Haerter. *International Conference Fires in Tunnels*, pages 195–214. 1994.

[46] Sung Ryong Lee and Hong Sun Ryou. A numerical study on smoke movement in longitudinal ventilation tunnel fires for different aspect ratio. *Building and Environment*, 41(6):719–725, 2006.

[47] Pollrich DLK Fan Factories. Tunnel jet fans the basic series.

[48] Daniel Swenson. Modeling jet fans, part 2: Validation using experimental data, 2016.

[49] K McGrattan, S. Hostikka, Randall McDermott, Jason Floyd, Craig Weinschenk, and Kristopher Overholt. Sixth Edition Fire Dynamics Simulator Technical Reference Guide Volume 2 : Verification. 2, 2016.

[50] L. Prahl, A. Hölzer, D. Arlov, J. Revstedt, M. Sommerfeld, and L. Fuchs. On the interaction between two fixed spherical particles. *International Journal of Multiphase Flow*, 33(7):707–725, 2007.

[51] Jukka Vaari, Simo Hostikka, Topi Sikanen, and Antti Paajanen. *Numerical simulations on the performance of waterbased fire suppressions systems.* 2012.

[52] Elizabeth Blanchard, É Cole D Octorale, and Emma Ed. Computational study of water mist for a tunnel fire application to be presented at Computational study of water mist for a tunnel fire application. 2013.

[53] Karlsson Bjrn and James G. Quintiere. *Enclosure fire dynamics.* CRC Press, 2000.

Appendix

FDS Codes

Example: Scenario without Fire

```
nofire_h35_5w.fds
Generated by PyroSim - Version 2017.2.1115
05-Mar-2018 15:58:07

&HEAD CHID='nofire_h35_5w'/
&TIME T_END=500.0/
&DUMP RENDER_FILE='nofire_h35_5w.ge1', MAXIMUM_PARTICLES=15000000, DT_DEVC=5.0,
DT_SLCF=10.0/

&MESH ID='1', IJK=48,8,7, XB=-120.0,-72.0,-1.0,7.0,0.0,7.0, MPI_PROCESS=0/
&MESH ID='3', IJK=387,8,7, XB=113.0,500.0,-1.0,7.0,0.0,7.0, MPI_PROCESS=0/
&MESH ID='BUFFER', IJK=45,16,14, XB=90.5,113.0,-1.0,7.0,0.0,7.0, MPI_PROCESS=0/
&MESH ID='JET', IJK=303,16,14, XB=-72.0,79.5,-1.0,7.0,0.0,7.0, MPI_PROCESS=1/
&MESH ID='FIRE', IJK=44,32,28, XB=79.5,90.5,-1.0,7.0,0.0,7.0, MPI_PROCESS=2/


&SPEC ID='WATER VAPOR SPK', SPEC_ID='WATER VAPOR'/

&PART ID='WATER MIST',
    SPEC_ID='WATER VAPOR SPK',
    DIAMETER=200.0/

&PROP ID='WATER MIST',
    PART_ID='WATER MIST',
    K_FACTOR=4.3,
    OPERATING_PRESSURE=40.0,
    PARTICLE_VELOCITY=15.0,
    SPRAY_ANGLE=30.0,80.0/

&DEVC ID='U-UP_0m_0', QUANTITY='U-VELOCITY', XYZ=70.5,0.5,0.25/
&DEVC ID='U-UP_0m_1', QUANTITY='U-VELOCITY', XYZ=70.5,1.5,0.25/
&DEVC ID='U-UP_0m_2', QUANTITY='U-VELOCITY', XYZ=70.5,2.5,0.25/
&DEVC ID='U-UP_0m_3', QUANTITY='U-VELOCITY', XYZ=70.5,3.5,0.25/
&DEVC ID='U-UP_0m_4', QUANTITY='U-VELOCITY', XYZ=70.5,4.5,0.25/
&DEVC ID='U-UP_0m_5', QUANTITY='U-VELOCITY', XYZ=70.5,5.5,0.25/
&DEVC ID='U-UP_1m_0', QUANTITY='U-VELOCITY', XYZ=70.5,0.5,1.25/
&DEVC ID='U-UP_1m_1', QUANTITY='U-VELOCITY', XYZ=70.5,1.5,1.25/
&DEVC ID='U-UP_1m_2', QUANTITY='U-VELOCITY', XYZ=70.5,2.5,1.25/
&DEVC ID='U-UP_1m_3', QUANTITY='U-VELOCITY', XYZ=70.5,3.5,1.25/
&DEVC ID='U-UP_1m_4', QUANTITY='U-VELOCITY', XYZ=70.5,4.5,1.25/
&DEVC ID='U-UP_1m_5', QUANTITY='U-VELOCITY', XYZ=70.5,5.5,1.25/
&DEVC ID='U-UP_2m_0', QUANTITY='U-VELOCITY', XYZ=70.5,0.5,2.25/
&DEVC ID='U-UP_2m_1', QUANTITY='U-VELOCITY', XYZ=70.5,1.5,2.25/
&DEVC ID='U-UP_2m_2', QUANTITY='U-VELOCITY', XYZ=70.5,2.5,2.25/
&DEVC ID='U-UP_2m_3', QUANTITY='U-VELOCITY', XYZ=70.5,3.5,2.25/
&DEVC ID='U-UP_2m_4', QUANTITY='U-VELOCITY', XYZ=70.5,4.5,2.25/
&DEVC ID='U-UP_2m_5', QUANTITY='U-VELOCITY', XYZ=70.5,5.5,2.25/
&DEVC ID='U-UP_3m_0', QUANTITY='U-VELOCITY', XYZ=70.5,0.5,3.25/
&DEVC ID='U-UP_3m_1', QUANTITY='U-VELOCITY', XYZ=70.5,1.5,3.25/
&DEVC ID='U-UP_3m_2', QUANTITY='U-VELOCITY', XYZ=70.5,2.5,3.25/
&DEVC ID='U-UP_3m_3', QUANTITY='U-VELOCITY', XYZ=70.5,3.5,3.25/
&DEVC ID='U-UP_3m_4', QUANTITY='U-VELOCITY', XYZ=70.5,4.5,3.25/
&DEVC ID='U-UP_3m_5', QUANTITY='U-VELOCITY', XYZ=70.5,5.5,3.25/
&DEVC ID='U-UP_4m_0', QUANTITY='U-VELOCITY', XYZ=70.5,0.5,4.25/
&DEVC ID='U-UP_4m_1', QUANTITY='U-VELOCITY', XYZ=70.5,1.5,4.25/
&DEVC ID='U-UP_4m_2', QUANTITY='U-VELOCITY', XYZ=70.5,2.5,4.25/
&DEVC ID='U-UP_4m_3', QUANTITY='U-VELOCITY', XYZ=70.5,3.5,4.25/
```

```
&DEVC ID='U-UP_4m_4', QUANTITY='U-VELOCITY', XYZ=70.5,4.5,4.25/
&DEVC ID='U-UP_4m_5', QUANTITY='U-VELOCITY', XYZ=70.5,5.5,4.25/
&DEVC ID='U-UP_5m_0', QUANTITY='U-VELOCITY', XYZ=70.5,0.5,5.25/
&DEVC ID='U-UP_5m_1', QUANTITY='U-VELOCITY', XYZ=70.5,1.5,5.25/
&DEVC ID='U-UP_5m_2', QUANTITY='U-VELOCITY', XYZ=70.5,2.5,5.25/
&DEVC ID='U-UP_5m_3', QUANTITY='U-VELOCITY', XYZ=70.5,3.5,5.25/
&DEVC ID='U-UP_5m_4', QUANTITY='U-VELOCITY', XYZ=70.5,4.5,5.25/
&DEVC ID='U-UP_5m_5', QUANTITY='U-VELOCITY', XYZ=70.5,5.5,5.25/

&DEVC ID='WATER MIST 1', PROP_ID='WATER MIST', XYZ=79.0,3.0,5.5, QUANTITY='TIME',
SETPOINT=0.0/
&DEVC ID='WATER MIST 2', PROP_ID='WATER MIST', XYZ=82.0,3.0,5.5, QUANTITY='TIME',
SETPOINT=0.0/
&DEVC ID='WATER MIST 3', PROP_ID='WATER MIST', XYZ=85.0,3.0,5.5, QUANTITY='TIME',
SETPOINT=0.0/
&DEVC ID='WATER MIST 4', PROP_ID='WATER MIST', XYZ=88.0,3.0,5.5, QUANTITY='TIME',
SETPOINT=0.0/
&DEVC ID='WATER MIST 5', PROP_ID='WATER MIST', XYZ=91.0,3.0,5.5, QUANTITY='TIME',
SETPOINT=0.0/


&OBST ID='\par', XB=-100.0,500.0,-1.0,0.0,0.0,6.0, COLOR='GRAY 60', SURF_ID='INERT'/
&OBST ID='\par', XB=-100.0,500.0,6.0,7.0,0.0,6.0, COLOR='GRAY 60', SURF_ID='INERT'/
&OBST ID='\par', XB=-100.0,500.0,-1.0,7.0,6.0,7.0, COLOR='GRAY 60', SURF_ID='INERT'/
&OBST ID='HGV\par', XB=80.0,90.0,1.5,4.5,1.0,3.5, COLOR='GRAY 60', SURF_ID='INERT'/
&OBST ID='JET FAN 1\par', XB=27.0,29.0,0.5,1.5,4.5,5.5, RGB=51,102,255, SURF_ID='INERT'/
&OBST ID='JET FAN 3\par', XB=27.0,29.0,4.5,5.5,4.5,5.5, RGB=51,102,255, SURF_ID='INERT'/
&OBST ID='JET FAN 2\par', XB=27.0,29.0,2.5,3.5,4.5,5.5, RGB=51,102,255, SURF_ID='INERT'/
&OBST ID='JET FAN 1 SHROUD', XB=29.0,30.0,0.5,0.5,4.5,5.5, RGB=51,102,255, SURF_ID='INERT'/
&OBST ID='JET FAN 1 SHROUD', XB=29.0,30.0,0.5,1.5,5.5,5.5, RGB=51,102,255, SURF_ID='INERT'/
&OBST ID='JET FAN 1 SHROUD', XB=29.0,30.0,0.5,1.5,4.5,4.5, RGB=51,102,255, SURF_ID='INERT'/
&OBST ID='JET FAN 1 SHROUD', XB=29.0,30.0,1.5,1.5,4.5,5.5, RGB=51,102,255, SURF_ID='INERT'/
&OBST ID='JET FAN 2 SHROUD', XB=29.0,30.0,2.5,2.5,4.5,5.5, RGB=51,102,255, SURF_ID='INERT'/
&OBST ID='JET FAN 2 SHROUD', XB=29.0,30.0,3.5,3.5,4.5,5.5, RGB=51,102,255, SURF_ID='INERT'/
&OBST ID='JET FAN 2 SHROUD', XB=29.0,30.0,2.5,3.5,5.5,5.5, RGB=51,102,255, SURF_ID='INERT'/
&OBST ID='JET FAN 2 SHROUD', XB=29.0,30.0,2.5,3.5,4.5,4.5, RGB=51,102,255, SURF_ID='INERT'/
&OBST ID='JET FAN 3 SHROUD', XB=29.0,30.0,4.5,4.5,4.5,5.5, RGB=51,102,255, SURF_ID='INERT'/
&OBST ID='JET FAN 3 SHROUD', XB=29.0,30.0,5.5,5.5,4.5,5.5, RGB=51,102,255, SURF_ID='INERT'/
&OBST ID='JET FAN 3 SHROUD', XB=29.0,30.0,4.5,5.5,5.5,5.5, RGB=51,102,255, SURF_ID='INERT'/
&OBST ID='JET FAN 3 SHROUD', XB=29.0,30.0,4.5,5.5,4.5,4.5, RGB=51,102,255, SURF_ID='INERT'/


&VENT ID='Mesh Vent: 1 [XMIN]', SURF_ID='OPEN', XB=-120.0,-120.0,-1.0,7.0,0.0,7.0/
&VENT ID='Mesh Vent: 3 [XMAX]', SURF_ID='OPEN', XB=500.0,500.0,-1.0,7.0,0.0,7.0/
&VENT ID='LEAK', SURF_ID='OPEN', XB=76.0,76.5,2.0,2.5,0.0,0.0/
&VENT ID='OUT1', SURF_ID='HVAC', XB=29.0,29.0,0.5,1.5,4.5,5.5, COLOR='BLUE'/
&VENT ID='OUT2', SURF_ID='HVAC', XB=29.0,29.0,2.5,3.5,4.5,5.5, COLOR='BLUE'/
&VENT ID='IN3', SURF_ID='HVAC', XB=27.0,27.0,4.5,5.5,4.5,5.5, COLOR='BLUE'/
&VENT ID='IN2', SURF_ID='HVAC', XB=27.0,27.0,2.5,3.5,4.5,5.5, COLOR='BLUE'/
&VENT ID='IN1', SURF_ID='HVAC', XB=27.0,27.0,0.5,1.5,4.5,5.5, COLOR='BLUE'/
&VENT ID='OUT3', SURF_ID='HVAC', XB=29.0,29.0,4.5,5.5,4.5,5.5, COLOR='BLUE'/

&HVAC ID='IN1', TYPE_ID='NODE', DUCT_ID='JET FAN 1', VENT_ID='IN1'/
&HVAC ID='OUT1', TYPE_ID='NODE', DUCT_ID='JET FAN 1', VENT_ID='OUT1'/
&HVAC ID='JET FAN 1', TYPE_ID='DUCT', DIAMETER=0.84, VOLUME_FLOW=16.9,
NODE_ID='IN1','OUT1', ROUGHNESS=1.0E-3, LENGTH=2.0/
&HVAC ID='OUT2', TYPE_ID='NODE', DUCT_ID='JET FAN 2', VENT_ID='OUT2'/
&HVAC ID='OUT3', TYPE_ID='NODE', DUCT_ID='JET FAN 3', VENT_ID='OUT3'/
&HVAC ID='JET FAN 2', TYPE_ID='DUCT', DIAMETER=0.84, VOLUME_FLOW=16.9,
```

```
NODE_ID='IN2','OUT2', ROUGHNESS=1.0E-3, LENGTH=2.0/
&HVAC ID='JET FAN 3', TYPE_ID='DUCT', DIAMETER=0.84, VOLUME_FLOW=16.9,
NODE_ID='IN3','OUT3', ROUGHNESS=1.0E-3, LENGTH=2.0/
&HVAC ID='IN3', TYPE_ID='NODE', DUCT_ID='JET FAN 3', VENT_ID='IN3'/
&HVAC ID='IN2', TYPE_ID='NODE', DUCT_ID='JET FAN 2', VENT_ID='IN2'/

&SLCF QUANTITY='TEMPERATURE', VECTOR=.TRUE., PBY=3.0/
&SLCF QUANTITY='TEMPERATURE', VECTOR=.TRUE., PBY=1.0/
&SLCF QUANTITY='TEMPERATURE', VECTOR=.TRUE., PBY=5.0/
&SLCF QUANTITY='TEMPERATURE', VECTOR=.TRUE., PBZ=1.0/
&SLCF QUANTITY='TEMPERATURE', VECTOR=.TRUE., PBZ=2.0/
&SLCF QUANTITY='TEMPERATURE', VECTOR=.TRUE., PBZ=3.0/
&SLCF QUANTITY='TEMPERATURE', VECTOR=.TRUE., PBZ=4.0/
&SLCF QUANTITY='TEMPERATURE', VECTOR=.TRUE., PBZ=5.0/
&SLCF QUANTITY='TEMPERATURE', VECTOR=.TRUE., PBZ=5.5/
&SLCF QUANTITY='VELOCITY', VECTOR=.TRUE., PBZ=5.5/
&SLCF QUANTITY='U-VELOCITY', VECTOR=.TRUE., PBZ=5.5/
&SLCF QUANTITY='VELOCITY', VECTOR=.TRUE., PBZ=4.5/
&SLCF QUANTITY='U-VELOCITY', VECTOR=.TRUE., PBZ=4.5/
&SLCF QUANTITY='VELOCITY', VECTOR=.TRUE., PBZ=3.5/
&SLCF QUANTITY='U-VELOCITY', VECTOR=.TRUE., PBZ=3.5/
&SLCF QUANTITY='VELOCITY', VECTOR=.TRUE., PBZ=2.5/
&SLCF QUANTITY='U-VELOCITY', VECTOR=.TRUE., PBZ=2.5/
&SLCF QUANTITY='VELOCITY', VECTOR=.TRUE., PBZ=1.5/
&SLCF QUANTITY='U-VELOCITY', VECTOR=.TRUE., PBZ=1.5/
&SLCF QUANTITY='U-VELOCITY', VECTOR=.TRUE., PBY=3.0/
&SLCF QUANTITY='U-VELOCITY', VECTOR=.TRUE., PBY=1.0/
&SLCF QUANTITY='U-VELOCITY', VECTOR=.TRUE., PBY=5.0/


&TAIL /
```

Example: Base Case Scenario

v40MW_h45_10w_final.fds
Generated by PyroSim - Version 2017.2.1115
02-Apr-2018 16:18:24

```
&HEAD CHID='v40MW_h45_10w_final'/
&TIME T_END=1000.0/
&DUMP RENDER_FILE='v40MW_h45_10w_final.ge1', MAXIMUM_PARTICLES=15000000,
DT_DEVC=5.0, DT_SLCF=10.0/

&MESH ID='1', IJK=48,8,7, XB=-120.0,-72.0,-1.0,7.0,0.0,7.0, MPI_PROCESS=0/
&MESH ID='3', IJK=387,8,7, XB=113.0,500.0,-1.0,7.0,0.0,7.0, MPI_PROCESS=0/
&MESH ID='BUFFER', IJK=45,16,14, XB=90.5,113.0,-1.0,7.0,0.0,7.0, MPI_PROCESS=0/
&MESH ID='JET', IJK=303,16,14, XB=-72.0,79.5,-1.0,7.0,0.0,7.0, MPI_PROCESS=1/
&MESH ID='FIRE', IJK=44,32,18, XB=79.5,90.5,-1.0,7.0,0.0,4.5, MPI_PROCESS=2/
&MESH ID='FIRE-2', IJK=44,16,10, XB=79.5,90.5,-1.0,3.0,4.5,7.0, MPI_PROCESS=3/
&MESH ID='FIRE-4', IJK=44,16,10, XB=79.5,90.5,3.0,7.0,4.5,7.0, MPI_PROCESS=4/


&SPEC ID='WATER VAPOR SPK', SPEC_ID='WATER VAPOR'/

&PART ID='WATER MIST',
     SPEC_ID='WATER VAPOR SPK',
     DIAMETER=200.0/

&REAC ID='HGV',
     FUEL='REAC_FUEL',
     C=1.0,
     H=2.0,
     O=0.62,
     CO_YIELD=0.012,
     SOOT_YIELD=0.012,
     HEAT_OF_COMBUSTION=2.0E4/

&PROP ID='WATER MIST',
     PART_ID='WATER MIST',
     K_FACTOR=4.3,
     OPERATING_PRESSURE=40.0,
     PARTICLE_VELOCITY=15.0,
     SPRAY_ANGLE=30.0,80.0/

&DEVC ID='SPK H20_1', QUANTITY='DENSITY', SPEC_ID='WATER VAPOR SPK',
STATISTICS='VOLUME INTEGRAL', XB=-72.0,79.5,-1.0,7.0,0.0,7.0/
&DEVC ID='SPK H20_2', QUANTITY='DENSITY', SPEC_ID='WATER VAPOR SPK',
STATISTICS='VOLUME INTEGRAL', XB=79.5,90.5,-1.0,7.0,0.0,4.5/
&DEVC ID='SPK H20_3', QUANTITY='DENSITY', SPEC_ID='WATER VAPOR SPK',
STATISTICS='VOLUME INTEGRAL', XB=79.5,90.5,-1.0,3.0,4.5,7.0/
&DEVC ID='SPK H20_4', QUANTITY='DENSITY', SPEC_ID='WATER VAPOR SPK',
STATISTICS='VOLUME INTEGRAL', XB=79.5,90.5,3.0,7.0,4.5,7.0/
&DEVC ID='SPK H20_5', QUANTITY='DENSITY', SPEC_ID='WATER VAPOR SPK',
STATISTICS='VOLUME INTEGRAL', XB=90.5,113.0,-1.0,7.0,0.0,7.0/


&DEVC ID='Soot_79m_01', QUANTITY='MASS FRACTION', SPEC_ID='SOOT', XYZ=79.25,0.25,5.75/
&DEVC ID='Soot_79m_1', QUANTITY='MASS FRACTION', SPEC_ID='SOOT', XYZ=79.25,1.25,5.75/
&DEVC ID='Soot_79m_2', QUANTITY='MASS FRACTION', SPEC_ID='SOOT', XYZ=79.25,2.25,5.75/
&DEVC ID='Soot_79m_3', QUANTITY='MASS FRACTION', SPEC_ID='SOOT', XYZ=79.25,3.25,5.75/
```

&DEVC ID='Soot_79m_4', QUANTITY='MASS FRACTION', SPEC_ID='SOOT', XYZ=79.25,4.25,5.75/
&DEVC ID='Soot_79m_5', QUANTITY='MASS FRACTION', SPEC_ID='SOOT', XYZ=79.25,5.25,5.75/
&DEVC ID='U-UP_1m_0', QUANTITY='U-VELOCITY', XYZ=70.5,0.5,1.25/
&DEVC ID='U-UP_1m_1', QUANTITY='U-VELOCITY', XYZ=70.5,1.5,1.25/
&DEVC ID='U-UP_1m_2', QUANTITY='U-VELOCITY', XYZ=70.5,2.5,1.25/
&DEVC ID='U-UP_1m_3', QUANTITY='U-VELOCITY', XYZ=70.5,3.5,1.25/
&DEVC ID='U-UP_1m_4', QUANTITY='U-VELOCITY', XYZ=70.5,4.5,1.25/
&DEVC ID='U-UP_1m_5', QUANTITY='U-VELOCITY', XYZ=70.5,5.5,1.25/
&DEVC ID='U-UP_2m_0', QUANTITY='U-VELOCITY', XYZ=70.5,0.5,2.25/
&DEVC ID='U-UP_2m_1', QUANTITY='U-VELOCITY', XYZ=70.5,1.5,2.25/
&DEVC ID='U-UP_2m_2', QUANTITY='U-VELOCITY', XYZ=70.5,2.5,2.25/
&DEVC ID='U-UP_2m_3', QUANTITY='U-VELOCITY', XYZ=70.5,3.5,2.25/
&DEVC ID='U-UP_2m_4', QUANTITY='U-VELOCITY', XYZ=70.5,4.5,2.25/
&DEVC ID='U-UP_2m_5', QUANTITY='U-VELOCITY', XYZ=70.5,5.5,2.25/
&DEVC ID='U-UP_3m_0', QUANTITY='U-VELOCITY', XYZ=70.5,0.5,3.25/
&DEVC ID='U-UP_3m_1', QUANTITY='U-VELOCITY', XYZ=70.5,1.5,3.25/
&DEVC ID='U-UP_3m_2', QUANTITY='U-VELOCITY', XYZ=70.5,2.5,3.25/
&DEVC ID='U-UP_3m_3', QUANTITY='U-VELOCITY', XYZ=70.5,3.5,3.25/
&DEVC ID='U-UP_3m_4', QUANTITY='U-VELOCITY', XYZ=70.5,4.5,3.25/
&DEVC ID='U-UP_3m_5', QUANTITY='U-VELOCITY', XYZ=70.5,5.5,3.25/
&DEVC ID='U-UP_4m_0', QUANTITY='U-VELOCITY', XYZ=70.5,0.5,4.25/
&DEVC ID='U-UP_4m_1', QUANTITY='U-VELOCITY', XYZ=70.5,1.5,4.25/
&DEVC ID='U-UP_4m_2', QUANTITY='U-VELOCITY', XYZ=70.5,2.5,4.25/
&DEVC ID='U-UP_4m_3', QUANTITY='U-VELOCITY', XYZ=70.5,3.5,4.25/
&DEVC ID='U-UP_4m_4', QUANTITY='U-VELOCITY', XYZ=70.5,4.5,4.25/
&DEVC ID='U-UP_4m_5', QUANTITY='U-VELOCITY', XYZ=70.5,5.5,4.25/
&DEVC ID='U-UP_5m_0', QUANTITY='U-VELOCITY', XYZ=70.5,0.5,5.25/
&DEVC ID='U-UP_5m_1', QUANTITY='U-VELOCITY', XYZ=70.5,1.5,5.25/
&DEVC ID='U-UP_5m_2', QUANTITY='U-VELOCITY', XYZ=70.5,2.5,5.25/
&DEVC ID='U-UP_5m_3', QUANTITY='U-VELOCITY', XYZ=70.5,3.5,5.25/
&DEVC ID='U-UP_5m_4', QUANTITY='U-VELOCITY', XYZ=70.5,4.5,5.25/
&DEVC ID='U-UP_5m_5', QUANTITY='U-VELOCITY', XYZ=70.5,5.5,5.25/

&DEVC ID='Soot_78m_01', QUANTITY='MASS FRACTION', SPEC_ID='SOOT', XYZ=78.25,0.25,5.75/
&DEVC ID='Soot_78m_1', QUANTITY='MASS FRACTION', SPEC_ID='SOOT', XYZ=78.25,1.25,5.75/
&DEVC ID='Soot_78m_2', QUANTITY='MASS FRACTION', SPEC_ID='SOOT', XYZ=78.25,2.25,5.75/
&DEVC ID='Soot_78m_3', QUANTITY='MASS FRACTION', SPEC_ID='SOOT', XYZ=78.25,3.25,5.75/
&DEVC ID='Soot_78m_4', QUANTITY='MASS FRACTION', SPEC_ID='SOOT', XYZ=78.25,4.25,5.75/
&DEVC ID='Soot_78m_5', QUANTITY='MASS FRACTION', SPEC_ID='SOOT', XYZ=78.25,5.25,5.75/
&DEVC ID='Soot_77m_01', QUANTITY='MASS FRACTION', SPEC_ID='SOOT', XYZ=77.25,0.25,5.75/
&DEVC ID='Soot_77m_1', QUANTITY='MASS FRACTION', SPEC_ID='SOOT', XYZ=77.25,1.25,5.75/
&DEVC ID='Soot_77m_2', QUANTITY='MASS FRACTION', SPEC_ID='SOOT', XYZ=77.25,2.25,5.75/
&DEVC ID='Soot_77m_3', QUANTITY='MASS FRACTION', SPEC_ID='SOOT', XYZ=77.25,3.25,5.75/
&DEVC ID='Soot_77m_4', QUANTITY='MASS FRACTION', SPEC_ID='SOOT', XYZ=77.25,4.25,5.75/
&DEVC ID='Soot_77m_5', QUANTITY='MASS FRACTION', SPEC_ID='SOOT', XYZ=77.25,5.25,5.75/
&DEVC ID='Soot_76m_01', QUANTITY='MASS FRACTION', SPEC_ID='SOOT', XYZ=76.25,0.25,5.75/
&DEVC ID='Soot_76m_1', QUANTITY='MASS FRACTION', SPEC_ID='SOOT', XYZ=76.25,1.25,5.75/
&DEVC ID='Soot_76m_2', QUANTITY='MASS FRACTION', SPEC_ID='SOOT', XYZ=76.25,2.25,5.75/
&DEVC ID='Soot_76m_3', QUANTITY='MASS FRACTION', SPEC_ID='SOOT', XYZ=76.25,3.25,5.75/
&DEVC ID='Soot_76m_4', QUANTITY='MASS FRACTION', SPEC_ID='SOOT', XYZ=76.25,4.25,5.75/
&DEVC ID='Soot_76m_5', QUANTITY='MASS FRACTION', SPEC_ID='SOOT', XYZ=76.25,5.25,5.75/
&DEVC ID='Soot_75m_01', QUANTITY='MASS FRACTION', SPEC_ID='SOOT', XYZ=75.25,0.25,5.75/
&DEVC ID='Soot_75m_1', QUANTITY='MASS FRACTION', SPEC_ID='SOOT', XYZ=75.25,1.25,5.75/
&DEVC ID='Soot_75m_2', QUANTITY='MASS FRACTION', SPEC_ID='SOOT', XYZ=75.25,2.25,5.75/
&DEVC ID='Soot_75m_3', QUANTITY='MASS FRACTION', SPEC_ID='SOOT', XYZ=75.25,3.25,5.75/
&DEVC ID='Soot_75m_4', QUANTITY='MASS FRACTION', SPEC_ID='SOOT', XYZ=75.25,4.25,5.75/
&DEVC ID='Soot_75m_5', QUANTITY='MASS FRACTION', SPEC_ID='SOOT', XYZ=75.25,5.25,5.75/

&DEVC ID='Soot2_79m_0', QUANTITY='MASS FRACTION', SPEC_ID='SOOT', XYZ=79.25,0.25,5.25/

&DEVC ID='Soot2_79m_01', QUANTITY='MASS FRACTION', SPEC_ID='SOOT', XYZ=79.25,1.25,5.25/
&DEVC ID='Soot2_79m_02', QUANTITY='MASS FRACTION', SPEC_ID='SOOT', XYZ=79.25,2.25,5.25/
&DEVC ID='Soot2_79m_03', QUANTITY='MASS FRACTION', SPEC_ID='SOOT', XYZ=79.25,3.25,5.25/
&DEVC ID='Soot2_79m_04', QUANTITY='MASS FRACTION', SPEC_ID='SOOT', XYZ=79.25,4.25,5.25/
&DEVC ID='Soot2_79m_05', QUANTITY='MASS FRACTION', SPEC_ID='SOOT', XYZ=79.25,5.25,5.25/
&DEVC ID='Soot2_78m_0', QUANTITY='MASS FRACTION', SPEC_ID='SOOT', XYZ=78.25,0.25,5.25/
&DEVC ID='Soot2_78m_01', QUANTITY='MASS FRACTION', SPEC_ID='SOOT', XYZ=78.25,1.25,5.25/
&DEVC ID='Soot2_78m_02', QUANTITY='MASS FRACTION', SPEC_ID='SOOT', XYZ=78.25,2.25,5.25/
&DEVC ID='Soot2_78m_03', QUANTITY='MASS FRACTION', SPEC_ID='SOOT', XYZ=78.25,3.25,5.25/
&DEVC ID='Soot2_78m_04', QUANTITY='MASS FRACTION', SPEC_ID='SOOT', XYZ=78.25,4.25,5.25/
&DEVC ID='Soot2_78m_05', QUANTITY='MASS FRACTION', SPEC_ID='SOOT', XYZ=78.25,5.25,5.25/
&DEVC ID='Soot2_77m_0', QUANTITY='MASS FRACTION', SPEC_ID='SOOT', XYZ=77.25,0.25,5.25/
&DEVC ID='Soot2_77m_01', QUANTITY='MASS FRACTION', SPEC_ID='SOOT', XYZ=77.25,1.25,5.25/
&DEVC ID='Soot2_77m_02', QUANTITY='MASS FRACTION', SPEC_ID='SOOT', XYZ=77.25,2.25,5.25/
&DEVC ID='Soot2_77m_03', QUANTITY='MASS FRACTION', SPEC_ID='SOOT', XYZ=77.25,3.25,5.25/
&DEVC ID='Soot2_77m_04', QUANTITY='MASS FRACTION', SPEC_ID='SOOT', XYZ=77.25,4.25,5.25/
&DEVC ID='Soot2_77m_05', QUANTITY='MASS FRACTION', SPEC_ID='SOOT', XYZ=77.25,5.25,5.25/
&DEVC ID='Soot2_76m_0', QUANTITY='MASS FRACTION', SPEC_ID='SOOT', XYZ=76.25,0.25,5.25/
&DEVC ID='Soot2_76m_01', QUANTITY='MASS FRACTION', SPEC_ID='SOOT', XYZ=76.25,1.25,5.25/
&DEVC ID='Soot2_76m_02', QUANTITY='MASS FRACTION', SPEC_ID='SOOT', XYZ=76.25,2.25,5.25/
&DEVC ID='Soot2_76m_03', QUANTITY='MASS FRACTION', SPEC_ID='SOOT', XYZ=76.25,3.25,5.25/
&DEVC ID='Soot2_76m_04', QUANTITY='MASS FRACTION', SPEC_ID='SOOT', XYZ=76.25,4.25,5.25/
&DEVC ID='Soot2_76m_05', QUANTITY='MASS FRACTION', SPEC_ID='SOOT', XYZ=76.25,5.25,5.25/
&DEVC ID='Soot2_75m_0', QUANTITY='MASS FRACTION', SPEC_ID='SOOT', XYZ=75.25,0.25,5.25/
&DEVC ID='Soot2_75m_01', QUANTITY='MASS FRACTION', SPEC_ID='SOOT', XYZ=75.25,1.25,5.25/
&DEVC ID='Soot2_75m_02', QUANTITY='MASS FRACTION', SPEC_ID='SOOT', XYZ=75.25,2.25,5.25/
&DEVC ID='Soot2_75m_03', QUANTITY='MASS FRACTION', SPEC_ID='SOOT', XYZ=75.25,3.25,5.25/
&DEVC ID='Soot2_75m_04', QUANTITY='MASS FRACTION', SPEC_ID='SOOT', XYZ=75.25,4.25,5.25/
&DEVC ID='Soot2_75m_05', QUANTITY='MASS FRACTION', SPEC_ID='SOOT', XYZ=75.25,5.25,5.25/

&DEVC ID='Soot3_79m_0', QUANTITY='MASS FRACTION', SPEC_ID='SOOT', XYZ=79.25,0.25,4.75/
&DEVC ID='Soot3_79m_1', QUANTITY='MASS FRACTION', SPEC_ID='SOOT', XYZ=79.25,1.25,4.75/
&DEVC ID='Soot3_79m_2', QUANTITY='MASS FRACTION', SPEC_ID='SOOT', XYZ=79.25,2.25,4.75/
&DEVC ID='Soot3_79m_3', QUANTITY='MASS FRACTION', SPEC_ID='SOOT', XYZ=79.25,3.25,4.75/
&DEVC ID='Soot3_79m_4', QUANTITY='MASS FRACTION', SPEC_ID='SOOT', XYZ=79.25,4.25,4.75/
&DEVC ID='Soot3_79m_5', QUANTITY='MASS FRACTION', SPEC_ID='SOOT', XYZ=79.25,5.25,4.75/
&DEVC ID='Soot3_78m_0', QUANTITY='MASS FRACTION', SPEC_ID='SOOT', XYZ=78.25,0.25,4.75/
&DEVC ID='Soot3_78m_1', QUANTITY='MASS FRACTION', SPEC_ID='SOOT', XYZ=78.25,1.25,4.75/
&DEVC ID='Soot3_78m_2', QUANTITY='MASS FRACTION', SPEC_ID='SOOT', XYZ=78.25,2.25,4.75/
&DEVC ID='Soot3_78m_3', QUANTITY='MASS FRACTION', SPEC_ID='SOOT', XYZ=78.25,3.25,4.75/
&DEVC ID='Soot3_78m_4', QUANTITY='MASS FRACTION', SPEC_ID='SOOT', XYZ=78.25,4.25,4.75/
&DEVC ID='Soot3_78m_5', QUANTITY='MASS FRACTION', SPEC_ID='SOOT', XYZ=78.25,5.25,4.75/
&DEVC ID='Soot3_77m_0', QUANTITY='MASS FRACTION', SPEC_ID='SOOT', XYZ=77.25,0.25,4.75/
&DEVC ID='Soot3_77m_1', QUANTITY='MASS FRACTION', SPEC_ID='SOOT', XYZ=77.25,1.25,4.75/
&DEVC ID='Soot3_77m_2', QUANTITY='MASS FRACTION', SPEC_ID='SOOT', XYZ=77.25,2.25,4.75/
&DEVC ID='Soot3_77m_3', QUANTITY='MASS FRACTION', SPEC_ID='SOOT', XYZ=77.25,3.25,4.75/
&DEVC ID='Soot3_77m_4', QUANTITY='MASS FRACTION', SPEC_ID='SOOT', XYZ=77.25,4.25,4.75/
&DEVC ID='Soot3_77m_5', QUANTITY='MASS FRACTION', SPEC_ID='SOOT', XYZ=77.25,5.25,4.75/
&DEVC ID='Soot3_76m_0', QUANTITY='MASS FRACTION', SPEC_ID='SOOT', XYZ=76.25,0.25,4.75/
&DEVC ID='Soot3_76m_1', QUANTITY='MASS FRACTION', SPEC_ID='SOOT', XYZ=76.25,1.25,4.75/
&DEVC ID='Soot3_76m_2', QUANTITY='MASS FRACTION', SPEC_ID='SOOT', XYZ=76.25,2.25,4.75/
&DEVC ID='Soot3_76m_3', QUANTITY='MASS FRACTION', SPEC_ID='SOOT', XYZ=76.25,3.25,4.75/
&DEVC ID='Soot3_76m_4', QUANTITY='MASS FRACTION', SPEC_ID='SOOT', XYZ=76.25,4.25,4.75/
&DEVC ID='Soot3_76m_5', QUANTITY='MASS FRACTION', SPEC_ID='SOOT', XYZ=76.25,5.25,4.75/
&DEVC ID='Soot3_75m_0', QUANTITY='MASS FRACTION', SPEC_ID='SOOT', XYZ=75.25,0.25,4.75/
&DEVC ID='Soot3_75m_1', QUANTITY='MASS FRACTION', SPEC_ID='SOOT', XYZ=75.25,1.25,4.75/
&DEVC ID='Soot3_75m_2', QUANTITY='MASS FRACTION', SPEC_ID='SOOT', XYZ=75.25,2.25,4.75/
&DEVC ID='Soot3_75m_3', QUANTITY='MASS FRACTION', SPEC_ID='SOOT', XYZ=75.25,3.25,4.75/
&DEVC ID='Soot3_75m_4', QUANTITY='MASS FRACTION', SPEC_ID='SOOT', XYZ=75.25,4.25,4.75/

```
&DEVC ID='Soot3_75m_5', QUANTITY='MASS FRACTION', SPEC_ID='SOOT', XYZ=75.25,5.25,4.75/

&DEVC ID='WATER MIST 1', PROP_ID='WATER MIST', XYZ=79.0,1.5,5.5, QUANTITY='TIME',
SETPOINT=0.0/
&DEVC ID='WATER MIST 2', PROP_ID='WATER MIST', XYZ=82.0,1.5,5.5, QUANTITY='TIME',
SETPOINT=0.0/
&DEVC ID='WATER MIST 3', PROP_ID='WATER MIST', XYZ=85.0,1.5,5.5, QUANTITY='TIME',
SETPOINT=0.0/
&DEVC ID='WATER MIST 4', PROP_ID='WATER MIST', XYZ=88.0,1.5,5.5, QUANTITY='TIME',
SETPOINT=0.0/
&DEVC ID='WATER MIST 5', PROP_ID='WATER MIST', XYZ=91.0,1.5,5.5, QUANTITY='TIME',
SETPOINT=0.0/
&DEVC ID='WATER MIST 6', PROP_ID='WATER MIST', XYZ=79.0,4.5,5.5, QUANTITY='TIME',
SETPOINT=0.0/
&DEVC ID='WATER MIST 7', PROP_ID='WATER MIST', XYZ=82.0,4.5,5.5, QUANTITY='TIME',
SETPOINT=0.0/
&DEVC ID='WATER MIST 8', PROP_ID='WATER MIST', XYZ=85.0,4.5,5.5, QUANTITY='TIME',
SETPOINT=0.0/
&DEVC ID='WATER MIST 9', PROP_ID='WATER MIST', XYZ=88.0,4.5,5.5, QUANTITY='TIME',
SETPOINT=0.0/
&DEVC ID='WATER MIST 10', PROP_ID='WATER MIST', XYZ=91.0,4.5,5.5, QUANTITY='TIME',
SETPOINT=0.0/

&SURF ID='FIRE',
     FYI='100MW',
     COLOR='RED',
     HRRPUA=666.7/

&OBST ID='\par', XB=-100.0,500.0,-1.0,0.0,0.0,6.0, COLOR='GRAY 60', SURF_ID='INERT'/
&OBST ID='\par', XB=-100.0,500.0,6.0,7.0,0.0,6.0, COLOR='GRAY 60', SURF_ID='INERT'/
&OBST ID='\par', XB=-100.0,500.0,-1.0,7.0,6.0,7.0, COLOR='INVISIBLE', SURF_ID='INERT'/
&OBST ID='HGV\par', XB=80.0,90.0,1.5,4.5,1.0,4.5, COLOR='GRAY 60', SURF_ID='INERT'/
&OBST ID='JET FAN 1\par', XB=27.0,29.0,0.5,1.5,4.5,5.5, RGB=51,102,255, SURF_ID='INERT'/
&OBST ID='JET FAN 3\par', XB=27.0,29.0,4.5,5.5,4.5,5.5, RGB=51,102,255, SURF_ID='INERT'/
&OBST ID='JET FAN 2\par', XB=27.0,29.0,2.5,3.5,4.5,5.5, RGB=51,102,255, SURF_ID='INERT'/
&OBST ID='JET FAN 1 SHROUD', XB=29.0,30.0,0.5,0.5,4.5,5.5, RGB=51,102,255, SURF_ID='INERT'/
&OBST ID='JET FAN 1 SHROUD', XB=29.0,30.0,0.5,1.5,5.5,5.5, RGB=51,102,255, SURF_ID='INERT'/
&OBST ID='JET FAN 1 SHROUD', XB=29.0,30.0,0.5,1.5,4.5,4.5, RGB=51,102,255, SURF_ID='INERT'/
&OBST ID='JET FAN 1 SHROUD', XB=29.0,30.0,1.5,1.5,4.5,5.5, RGB=51,102,255, SURF_ID='INERT'/
&OBST ID='JET FAN 2 SHROUD', XB=29.0,30.0,2.5,2.5,4.5,5.5, RGB=51,102,255, SURF_ID='INERT'/
&OBST ID='JET FAN 2 SHROUD', XB=29.0,30.0,3.5,3.5,4.5,5.5, RGB=51,102,255, SURF_ID='INERT'/
&OBST ID='JET FAN 2 SHROUD', XB=29.0,30.0,2.5,3.5,5.5,5.5, RGB=51,102,255, SURF_ID='INERT'/
&OBST ID='JET FAN 2 SHROUD', XB=29.0,30.0,2.5,3.5,4.5,4.5, RGB=51,102,255, SURF_ID='INERT'/
&OBST ID='JET FAN 3 SHROUD', XB=29.0,30.0,4.5,4.5,4.5,5.5, RGB=51,102,255, SURF_ID='INERT'/
&OBST ID='JET FAN 3 SHROUD', XB=29.0,30.0,5.5,5.5,4.5,5.5, RGB=51,102,255, SURF_ID='INERT'/
&OBST ID='JET FAN 3 SHROUD', XB=29.0,30.0,4.5,5.5,5.5,5.5, RGB=51,102,255, SURF_ID='INERT'/
&OBST ID='JET FAN 3 SHROUD', XB=29.0,30.0,4.5,5.5,4.5,4.5, RGB=51,102,255, SURF_ID='INERT'/
&OBST ID='JET FAN 4', XB=-23.0,-21.0,0.5,1.5,4.5,5.5, RGB=51,102,255, SURF_ID='INERT'/
&OBST ID='JET FAN 4 SHROUD', XB=-21.0,-20.0,0.5,0.5,4.5,5.5, RGB=51,102,255, SURF_ID='INERT'/
&OBST ID='JET FAN 4 SHROUD', XB=-21.0,-20.0,0.5,1.5,5.5,5.5, RGB=51,102,255, SURF_ID='INERT'/
&OBST ID='JET FAN 4 SHROUD', XB=-21.0,-20.0,0.5,1.5,4.5,4.5, RGB=51,102,255, SURF_ID='INERT'/
&OBST ID='JET FAN 4 SHROUD', XB=-21.0,-20.0,1.5,1.5,4.5,5.5, RGB=51,102,255, SURF_ID='INERT'/
&OBST ID='JET FAN 5', XB=-23.0,-21.0,2.5,3.5,4.5,5.5, RGB=51,102,255, SURF_ID='INERT'/
&OBST ID='JET FAN 5 SHROUD', XB=-21.0,-20.0,2.5,2.5,4.5,5.5, RGB=51,102,255, SURF_ID='INERT'/
&OBST ID='JET FAN 5 SHROUD', XB=-21.0,-20.0,3.5,3.5,4.5,5.5, RGB=51,102,255, SURF_ID='INERT'/
&OBST ID='JET FAN 5 SHROUD', XB=-21.0,-20.0,2.5,3.5,5.5,5.5, RGB=51,102,255, SURF_ID='INERT'/
&OBST ID='JET FAN 5 SHROUD', XB=-21.0,-20.0,2.5,3.5,4.5,4.5, RGB=51,102,255, SURF_ID='INERT'/
&OBST ID='JET FAN 6', XB=-23.0,-21.0,4.5,5.5,4.5,5.5, RGB=51,102,255, SURF_ID='INERT'/
&OBST ID='JET FAN 6 SHROUD', XB=-21.0,-20.0,5.5,5.5,4.5,5.5, RGB=51,102,255, SURF_ID='INERT'/
```

```
&OBST ID='JET FAN 6 SHROUD', XB=-21.0,-20.0,4.5,5.5,5.5,5.5, RGB=51,102,255, SURF_ID='INERT'/
&OBST ID='JET FAN 6 SHROUD', XB=-21.0,-20.0,4.5,5.5,4.5,4.5, RGB=51,102,255, SURF_ID='INERT'/
&OBST ID='JET FAN 6 SHROUD', XB=-21.0,-20.0,4.5,4.5,4.5,5.5, RGB=51,102,255, SURF_ID='INERT'/

&VENT ID='Mesh Vent: 1 [XMIN]', SURF_ID='OPEN', XB=-120.0,-120.0,-1.0,7.0,0.0,7.0/
&VENT ID='Mesh Vent: 3 [XMAX]', SURF_ID='OPEN', XB=500.0,500.0,-1.0,7.0,0.0,7.0/
&VENT ID='LEAK', SURF_ID='OPEN', XB=76.0,76.5,2.0,2.5,0.0,0.0/
&VENT ID='Fire1', SURF_ID='FIRE', XB=80.0,90.0,1.5,1.5,3.0,4.5/
&VENT ID='Fire2', SURF_ID='FIRE', XB=80.0,90.0,4.5,4.5,3.0,4.5/
&VENT ID='Fire3', SURF_ID='FIRE', XB=80.0,90.0,1.5,4.5,4.5,4.5/
&VENT ID='OUT1', SURF_ID='HVAC', XB=29.0,29.0,0.5,1.5,4.5,5.5, COLOR='BLUE'/
&VENT ID='OUT2', SURF_ID='HVAC', XB=29.0,29.0,2.5,3.5,4.5,5.5, COLOR='BLUE'/
&VENT ID='IN3', SURF_ID='HVAC', XB=27.0,27.0,4.5,5.5,4.5,5.5, COLOR='BLUE'/
&VENT ID='IN2', SURF_ID='HVAC', XB=27.0,27.0,2.5,3.5,4.5,5.5, COLOR='BLUE'/
&VENT ID='IN1', SURF_ID='HVAC', XB=27.0,27.0,0.5,1.5,4.5,5.5, COLOR='BLUE'/
&VENT ID='OUT3', SURF_ID='HVAC', XB=29.0,29.0,4.5,5.5,4.5,5.5, COLOR='BLUE'/
&VENT ID='IN4', SURF_ID='HVAC', XB=-23.0,-23.0,0.5,1.5,4.5,5.5, COLOR='BLUE'/
&VENT ID='OUT4', SURF_ID='HVAC', XB=-21.0,-21.0,0.5,1.5,4.5,5.5, COLOR='BLUE'/
&VENT ID='IN5', SURF_ID='HVAC', XB=-23.0,-23.0,2.5,3.5,4.5,5.5, COLOR='BLUE'/
&VENT ID='OUT5', SURF_ID='HVAC', XB=-21.0,-21.0,2.5,3.5,4.5,5.5, COLOR='BLUE'/
&VENT ID='IN6', SURF_ID='HVAC', XB=-23.0,-23.0,4.5,5.5,4.5,5.5, COLOR='BLUE'/
&VENT ID='OUT6', SURF_ID='HVAC', XB=-21.0,-21.0,4.5,5.5,4.5,5.5, COLOR='BLUE'/

&HVAC ID='IN1', TYPE_ID='NODE', DUCT_ID='JET FAN 1', VENT_ID='IN1'/
&HVAC ID='OUT1', TYPE_ID='NODE', DUCT_ID='JET FAN 1', VENT_ID='OUT1'/
&HVAC ID='JET FAN 1', TYPE_ID='DUCT', DIAMETER=0.84, VOLUME_FLOW=16.9,
NODE_ID='IN1','OUT1', ROUGHNESS=1.0E-3, LENGTH=2.0/
&HVAC ID='OUT2', TYPE_ID='NODE', DUCT_ID='JET FAN 2', VENT_ID='OUT2'/
&HVAC ID='OUT3', TYPE_ID='NODE', DUCT_ID='JET FAN 3', VENT_ID='OUT3'/
&HVAC ID='JET FAN 2', TYPE_ID='DUCT', DIAMETER=0.84, VOLUME_FLOW=16.9,
NODE_ID='IN2','OUT2', ROUGHNESS=1.0E-3, LENGTH=2.0/
&HVAC ID='JET FAN 3', TYPE_ID='DUCT', DIAMETER=0.84, VOLUME_FLOW=16.9, RAMP_ID='JET
FAN 3_RAMP_ID', NODE_ID='IN3','OUT3', ROUGHNESS=1.0E-3, LENGTH=2.0/
&HVAC ID='IN3', TYPE_ID='NODE', DUCT_ID='JET FAN 3', VENT_ID='IN3'/
&HVAC ID='IN2', TYPE_ID='NODE', DUCT_ID='JET FAN 2', VENT_ID='IN2'/
&HVAC ID='IN4', TYPE_ID='NODE', DUCT_ID='JET FAN 4', VENT_ID='IN4'/
&HVAC ID='OUT4', TYPE_ID='NODE', DUCT_ID='JET FAN 4', VENT_ID='OUT4'/
&HVAC ID='JET FAN 4', TYPE_ID='DUCT', DIAMETER=0.84, VOLUME_FLOW=16.9, RAMP_ID='JET
FAN 4_RAMP_ID',NODE_ID='IN4','OUT4', ROUGHNESS=1.0E-3, LENGTH=2.0/
&HVAC ID='IN5', TYPE_ID='NODE', DUCT_ID='JET FAN 5', VENT_ID='IN5'/
&HVAC ID='OUT5', TYPE_ID='NODE', DUCT_ID='JET FAN 5', VENT_ID='OUT5'/
&HVAC ID='JET FAN 5', TYPE_ID='DUCT', DIAMETER=0.84, VOLUME_FLOW=16.9, RAMP_ID='JET
FAN 5_RAMP_ID',NODE_ID='IN5','OUT5', ROUGHNESS=1.0E-3, LENGTH=2.0/
&HVAC ID='IN6', TYPE_ID='NODE', DUCT_ID='JET FAN 6', VENT_ID='IN6'/
&HVAC ID='OUT6', TYPE_ID='NODE', DUCT_ID='JET FAN 6', VENT_ID='OUT6'/
&HVAC ID='JET FAN 6', TYPE_ID='DUCT', DIAMETER=0.84, VOLUME_FLOW=16.9, RAMP_ID='JET
FAN 6_RAMP_ID', NODE_ID='IN6','OUT6', ROUGHNESS=1.0E-3, LENGTH=2.0/

&RAMP ID='JET FAN 3_RAMP_ID', T=0.0, F=0.0/
&RAMP ID='JET FAN 3_RAMP_ID', T=300.0, F=0.0/
&RAMP ID='JET FAN 3_RAMP_ID', T=310.0, F=1.0/
&RAMP ID='JET FAN 3_RAMP_ID', T=1500.0, F=1.0/

&RAMP ID='JET FAN 4_RAMP_ID', T=0.0, F=0.0/
&RAMP ID='JET FAN 4_RAMP_ID', T=600.0, F=0.0/
&RAMP ID='JET FAN 4_RAMP_ID', T=610.0, F=1.0/
&RAMP ID='JET FAN 4_RAMP_ID', T=1500.0, F=1.0/

&RAMP ID='JET FAN 5_RAMP_ID', T=0.0, F=0.0/
```

```
&RAMP ID='JET FAN 5_RAMP_ID', T=900.0, F=0.0/
&RAMP ID='JET FAN 5_RAMP_ID', T=910.0, F=1.0/
&RAMP ID='JET FAN 5_RAMP_ID', T=1500.0, F=1.0/

&RAMP ID='JET FAN 6_RAMP_ID', T=0.0, F=0.0/
&RAMP ID='JET FAN 6_RAMP_ID', T=1200.0, F=0.0/
&RAMP ID='JET FAN 6_RAMP_ID', T=1210.0, F=1.0/
&RAMP ID='JET FAN 6_RAMP_ID', T=1500.0, F=1.0/

&SLCF QUANTITY='TEMPERATURE', PBY=3.0/
&SLCF QUANTITY='TEMPERATURE', PBY=1.0/
&SLCF QUANTITY='TEMPERATURE', PBY=5.0/
&SLCF QUANTITY='TEMPERATURE', PBZ=1.0/
&SLCF QUANTITY='TEMPERATURE', PBZ=2.0/
&SLCF QUANTITY='TEMPERATURE', PBZ=3.0/
&SLCF QUANTITY='TEMPERATURE', PBZ=4.0/
&SLCF QUANTITY='TEMPERATURE', PBZ=5.0/
&SLCF QUANTITY='TEMPERATURE', PBZ=5.5/
&SLCF QUANTITY='VELOCITY', VECTOR=.TRUE., PBZ=5.5/
&SLCF QUANTITY='U-VELOCITY', VECTOR=.TRUE., PBZ=5.5/
&SLCF QUANTITY='VELOCITY', VECTOR=.TRUE., PBZ=4.5/
&SLCF QUANTITY='U-VELOCITY', VECTOR=.TRUE., PBZ=4.5/
&SLCF QUANTITY='VELOCITY', VECTOR=.TRUE., PBZ=3.5/
&SLCF QUANTITY='U-VELOCITY', VECTOR=.TRUE., PBZ=3.5/
&SLCF QUANTITY='VELOCITY', VECTOR=.TRUE., PBZ=2.5/
&SLCF QUANTITY='U-VELOCITY', VECTOR=.TRUE., PBZ=2.5/
&SLCF QUANTITY='VELOCITY', VECTOR=.TRUE., PBZ=1.5/
&SLCF QUANTITY='U-VELOCITY', VECTOR=.TRUE., PBZ=1.5/
&SLCF QUANTITY='VELOCITY', VECTOR=.TRUE., PBY=3.0/
&SLCF QUANTITY='VELOCITY', VECTOR=.TRUE., PBY=1.0/
&SLCF QUANTITY='VELOCITY', VECTOR=.TRUE., PBY=5.0/
&SLCF QUANTITY='U-VELOCITY', VECTOR=.TRUE., PBY=3.0/
&SLCF QUANTITY='U-VELOCITY', VECTOR=.TRUE., PBY=1.0/
&SLCF QUANTITY='U-VELOCITY', VECTOR=.TRUE., PBY=5.0/
```